Geologica Acta, Vol.9, Nº 1, March 2011, 103-125
DOI: 10.1344/105.000001642
Available online at www.geologica-acta.com
geologica acta

Coexistence of calc-alkaline and ultrapotassic alkaline magmas at Mounts Cimini: evidence for transition from the Tuscan to the Roman Magmatic Provinces (Central Italy)

M. AULINAS [1] D. GASPERINI [1] [*] D. GIMENO [1] P. MACERA [2] J.L. FERNANDEZ-TURIEL [3] C. CIMARELLI [4]

[1] **Dept. de Geoquímica, Petrologia i Prospecció Geològica, Facultat de Geologia, Universitat de Barcelona (UB)**
Martí i Franquès s/n, 08028 Barcelona, Spain

[2] **Dipartimento di Scienze della Terra, Università di Pisa**
Via Santa Marta 33, 56126 Pisa, Italy

[3] **Institute of Earth Sciences J. Almera – CSIC**
Lluís Solé i Sabarís s/n, 08028 Barcelona, Spain

[4] **Dipartimento di Scienze Geologiche, Università di Roma 3**
Largo San Leonardo Murialdo 1, 00146 Rome, Italy

*Corresponding author: d.gasperini@dst.unipi.it
Phone +34 93 4021404; fax +34 93 4021340

ABSTRACT

The volcanic complex of Mts. Cimini (~0.90-1.30Ma) represents the geographical and chronological transition between the Tuscan Magmatic Province (TMP) and the Roman Magmatic Province (RMP), in central Italy. Major and trace elements, and Sr, Nd and Pb isotopes of whole-rock, as well as mineral chemistry analyses, were carried out on samples representative of the different petrographic and chronological units of Mts. Cimini. In particular, we focused on the olivine-bearing latites of Mts. Cimini that are the most mafic magmas, belong to the last phase of this volcanic activity, and are heterogeneous in highly incompatible element ratios and Sr-isotope compositions. We suggest that such heterogeneity reflects the occurrence of a heterogeneous upper mantle beneath central Italy, in which different portions, e.g., the sources of both the TMP and RMP, are characterized by distinct geochemical and petrographic features. In this scenario, about 900ka ago, the olivine-bearing latites mark the progressive decline of the TMP magma production in favour of partial melting of the RMP mantle region, thus recording the coexistence of both ultrapotassic alkaline and calc-alkaline magmas in the same volcanic region.

KEYWORDS | **Olivinlatite. Geochemistry. Ultrapotassic magmatism. Mantle heterogeneity. Mantle source.**

INTRODUCTION

The Tuscan Magmatic Province (TMP) and the Roman Magmatic Province (RMP) in central Italy have been proposed as a key magmatic region for the investigation of mantle and crust processes responsible for the broadly coeval coexistence of silica-oversaturated HK calc-alkaline and lamproite products (TMP) and ultrapotassic silica-undersaturated alkaline magmas (RMP) (e.g., Peccerillo et al., 1987; Peccerillo, 1999; Perini et al., 2000; Conticelli et al., 2002; Frezzotti et al., 2007). Silica-oversaturated rocks, abundant in the TMP, are characterized by a geochemical signature that is distinctive of magmas occurring in orogenic environments (Peccerillo et al., 1987; Serri et al., 1993, and references therein).

Ultrapotassic lavas are typical of the RMP and have been commonly related to metasomatism of the mantle by migration of selectively enriched fluids from recycled subducted material (e.g., Beccaluva et al., 1991; Conticelli and Peccerillo, 1992; Conticelli et al., 2002; Gasperini et al., 2002; Peccerillo, 2005).

The volcanic rocks of the TMP and RMP partly overlap with regard to their geochemical and isotopic compositions, and rocks with different K-enrichment coexist in the same volcanic center. Moreover, several studies suggest intimate relationships and interactions between the mantle sources of the TMP and RMP, due to mixing and/or mingling processes occurred at different depth in the local lithosphere (Serri et al., 1993; Peccerillo, 1999; Perini et al., 2000; Gasperini et al., 2002; Perini et al., 2003). In this view, a distinction between the TMP and RMP may be questionable, except for the geographical location of the volcanic activity.

Mounts Cimini volcanic center, while belonging to the TMP, was built up close to Vico volcano (RMP), and has been active up to about 0.52Ma before the debut of Vico volcanism (Nicoletti, 1969; Barberi et al., 1994; La Berge et al., 2004). Because of such geographical location and age, and for the coexistence of magmas with diverse alkali-affinity, this paper aims to evaluate if Mts. Cimini are suitable to investigate whether the TMP and RMP are distinct magmatic provinces or if a transition between the two can be chronologically and geochemically found.

GEOLOGICAL SETTING

The Plio-Pleistocene magmatism of the internal sector of the northern Apennine chain took place in a post-extensional tectonic setting, as the result of anticlockwise rotation of the Apennine chain within a back-arc extensional environment (Wilson, 1989; Beccaluva et al., 1991; Bartole, 1995; Giunchi et al., 1996; Serri, 1997; Argnani and Savelli, 1999; Meletti et al., 2000; Tamburelli et al., 2000; Peccerillo, 2005). At about 13 Ma, the Apennine collision terminated the westward subduction of the Adria plate under the European margin and rotated the direction of convergence to the northwest (Meletti et al., 2000). In the model of Wortel and Spakman (2000), a major discontinuity in the subducted slab is envisaged as "scissor type" faulting between the Ionian and Adriatic lithosphere. Due to gravitational forces, this tear migrated northwestward along the hinge of the subducted slab, ultimately resulting in a large slab window beneath the central-southern Apennines (see also Gasperini et al., 2002). Through such a tear, sub-lithospheric mantle material could have been channeled to the surface, contributing to the source of Italian mafic volcanism (Gasperini et al., 2002; Bianchini et al., 2008).

Geochronology

The small lamproitic outcrop at Sisco, North Corsica (about 14Ma; Bellon, 1981) is considered by most authors as the first magmatic event in this area (Civetta et al., 1978; Serri et al., 1993). After a large spatial and temporal gap, the oldest potassic magmatic activity in the Tuscan region occurred some 10My later (Orciatico and Montecatini Val di Cecina lamproites dated at 4.1Ma; Ferrara et al., 1989). Felsic intrusive and extrusive magmatism took place in southern Tuscany and in the Tuscan archipelago between 7.7 and 2.2Ma (Ferrara et al., 1988; Lombardi et al., 1974; Serri et al., 1993; Gasparon et al., 2009). Magmatism later migrated from west to east, with the sequential emplacement of Radicofani (1.3Ma; Innocenti et al., 1992), Cimini, and Torre Alfina (1.3–0.8Ma; Nicoletti, 1969; Fornaseri, 1985; Conticelli, 1998; La Berge et al., 2004) in the TMP. Potassic and ultrapotassic volcanism of the RMP began mainly in the upper Pleistocene (Barberi et al., 1991) and was characterized by the products of Vulsini (0.44-0.59 Ma; Cioni et al., 1993), Vico (0.42-0.09Ma; Laurenzi and Villa, 1987), Sabatini (0.60-0.43Ma; Cioni et al., 1993), Albani (0.6-0.02Ma; Scrocca et al., 2003), Ernici (0.25-0.15Ma; Scrocca et al., 2003) and Roccamonfina (0.63-0.13Ma; Scrocca et al., 2003). Notably, the magmatic activity of the RMP began at the end of Cimini and Torre Alfina (TMP) eruptive cycle.

Petrology and petrogenetic hypotheses

The TMP is characterized by the coexistence of both plutonic and volcanic rocks of sub-alkaline (acidic and high-K calc-alkaline or HKCA) to potassic alkaline (intermediate and acidic), and ultrapotassic (lamproites) affinities (Serri et al., 1993, and references therein). In contrast, the rocks from the RMP are exclusively volcanic and mostly comprise potassic alkaline compositions, even if significant amount of high-K calc-alkaline rocks

are buried under the potassic rocks in the Volturno plain (Campania; Beccaluva et al., 1991, 1994, 2005; Bianchini et al., 2008). The RMP rocks have been divided into the potassic (KS) and the highly potassic (HKS) series, on the basis of their K_2O/SiO_2 ratio (Marinelli, 1975; Foley et al., 1987; Serri et al., 1993; Beccaluva et al., 1994; Peccerillo, 1998; Gasperini et al., 2002; Perini et al., 2003; Frezzotti et al., 2007).

Calc-alkaline, shoshonitic and potassic rocks of the TMP and RMP are probably derived from anomalous mantle sources which were enriched in incompatible elements by subduction-related processes (e.g., Peccerillo and Manetti, 1985; Rogers et al., 1985; Ellam et al., 1989). The crust-derived component would result from melting of silicate metasedimentary rocks or sediments from a subducted slab. Gasperini et al. (2002) proposed that the crustal component is dominated by pelagic sediments, whereas CO_2-rich fluids released more recently by the incipient subduction of carbonate sedimentary rocks were identified by Conticelli et al. (2002) in the source of Italian potassic rocks. Alternatively, Avanzinelli et al. (2009) suggest that subduction of marly sediments with a variable carbonate fraction is a key component in the petrogenesis of the RMP rocks.

The age of mantle enrichment has implications for understanding the geodynamic evolution of the Tyrrhenian Sea and surrounding areas is ascribed to the Cenozoic orogenic cycle that ultimately led to the Apennine formation (Beccaluva et al., 1991, 1994, 2005; Bianchini et al., 2004; Peccerillo, 1999, 2002).

There is still no generals consensus about when it occurred, some 1-2Ga ago (e.g., Castorina et al., 2000) or during the Tertiary evolution of the Alpine-Apennine chains (Peccerillo, 1999, 2002).

Study area

Mounts Cimini

The Mts. Cimini complex is located in Latium (central Italy; Fig. 1), close to the Tyrrhenian margin, in a region affected by extensional dynamics related to the rifting of the Tyrrhenian Basin, which lead to the generation of a main NW-oriented graben and a series of NE-trending transversal grabens (Barberi et al., 1994; Cimarelli and De Rita, 2006). The volcanic complex is placed inside the Radicofani–Cimino graben (Fig. 1) and overlies Messinian-Quaternary sediments, Cretaceous–Eocene flysch and Meso-Cenozoic marly-carbonate rocks, which are superimposed on a low-grade metamorphic sedimentary basement (Sollevanti, 1983; Barberi et al., 1994; Perini et al., 2000).

Mts. Cimini are mainly characterized by highly silicic rocks of calc-alkaline nature, consisting of four main petrographic and chronological units, i.e., i) lava domes and ii) ignimbrites of trachyte-rhyodacite up to the limit of rhyolite composition, and minor low-silica iii) latitic and iv) olivine-bearing latite lavas (olivinlatites; Sollevanti, 1983; Innocenti et al., 1992; Aulinas et al., 2004).

Explosive activity followed shallow emplacement of lava domes and led to few ignimbrite deposits over an extension of ca. 300 km^2 (Puxeddu, 1971). This was followed by a final effusive activity, with the emplacement of latitic and olivinlatitic lavas (more than 8 km^2 and 6 km^2, respectively; Puxeddu, 1971).

$^{40}Ar/^{39}Ar$ data on sanidine crystals from lava domes gave an age of 1.330±0.013Ma, whereas $^{40}Ar/^{39}Ar$ data on sanidine from two ignimbrites gave a value of 1.30±0.01Ma (La Berge et al., 2004). These results are supported by new structural and stratigraphic data (Cimarelli and De Rita, 2006) which clearly indicate that the explosive activity (e.g., ignimbrite eruptions) at Mts. Cimini postdates the lava domes emplacement, as previously suggested by Sabatini (1912), Mittempergher and Tedesco (1963) and Lardini and Nappi (1987). The K-Ar age of olivinlatites

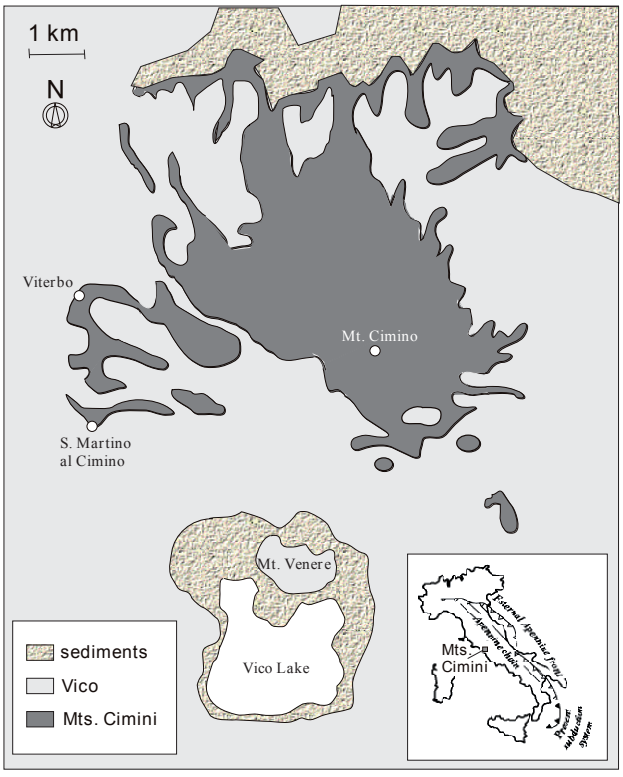

FIGURE 1 | **Sketch map showing the areal distribution of the volcanic products of Mts. Cimini and Vico, with respect to the location of the Vico lake on the caldera.**

is 0.95Ma (Nicoletti, 1969). Mts. Cimini magmas were subsequently covered by pyroclastic deposits belonging to the early Vico volcano activity.

Vico volcano

Vico volcano (0.42-0.09Ma; Laurenzi and Villa, 1985; Barberi et al., 1994) began its activity with plinian eruptions (Mattias and Ventriglia, 1970), accompanied by lava flows and trachyte domes. This was followed by several lava flows from the main crater, up to the building of the Vico stratovolcano. In this phase, early silica-saturated products (KS) were followed by larger volumes of more alkaline magmas (HKS), up to collapse of the stratovolcano. Post-caldera effusive and explosive activity occurred from different intra- and peri-caldera vents as well as from caldera fractures (Perini et al., 1997). During the last periods of activity, K-rich, mainly evolved, mildly to strongly silica undersaturated magmas were erupted (ignimbrites), leading to destruction of the volcanic edifice. Post caldera phreato-magmatic products are characterized by trachybasalts and latites (Bertagnini and Sbrana, 1986; Gasperini, 2003).

PETROGRAPHY AND MINERAL CHEMISTRY

The samples show variable textures from hypocrystalline pumices to hypohialine and holocrystalline lavas, with phenocryst contents ranging from 10-15% in the most basic lavas (olivinlatitic unit) to 20-25% in lava domes and ignimbrites.

The glomeroporphyric texture is common in dome and latitic lavas units, whereas vesicular texture is found in olivinlatites. Microlithes are frequent in the more recent units (latitic and olivinlatitic lavas) and perlitic texture is restricted to domes (Table 1). In the case of pyroclastites, welding is widespread and an eutaxitic texture is observed with a glassy groundmass describing a pseudofluidal texture.

In the most evolved samples (ignimbrites and lava dome units) the mineral assemblage includes sanidine, plagioclase, biotite, and orthopyroxene, with apatite and opaque minerals as accessory phases. Clinopyroxene and olivine are more frequent in the youngest lavas (latite and olivinlatite units), whereas sanidine, biotite and orthopyroxene and plagioclase are very rare. The mineral associations for the different chronostratigraphic units are reported in Table 1. Some of the studied lavas (independently of their chrono-stratigraphical unit) contain mafic xenoliths, the paragenesis of which mainly consists of plagioclase and orthopyroxene.

The mineral assemblage in a few lavas from Vico volcano shows textures similar to those of Mts. Cimini. One sample (V1) is characterized by abundant clinopyroxene, with minor plagioclase and scarce corroded sanidine and altered biotite. Conversely, samples MP33 and MP11 show centimetric subhedral sanidine crystals as the main mineral, with minor plagioclase and altered biotite, and rare clinopyroxene crystals.

Sanidine

Sanidine occurs within lava domes and ignimbrites, though it is also present in the latitic and especially in the olivinlatitic lavas. In the last two cases, the sanidine phenocrysts show clear evidence of disequilibrium, with rounded shape and corroded rims. All K-feldspar crystals are fairly homogeneous in composition (Or_{86}-Or_{72}), with the more potassic compositions found in olivinlatite lavas (Or_{86}-Or_{83}) (Table 2; Fig. 2). Analyses of sanidine from samples of the first period of magmatic activity at Vico volcano (RMP) show a wider compositional range (Or_{80}-Or_{64}) which is comparable to published data (Perini et al., 2000). Sanidine from Mts. Cimini show low BaO content (from 0.13 to 0.90 wt%) compared to those from the first erupted lavas of Vico (up to 3.40 wt% in our analyses; these finding are consistent with Perini et al., 2000).

Plagioclase

Plagioclase is present as pheno- and microcrysts. In lava domes and ignimbrites, they are euhedral to subhedral with normal An zoning. In contrast, the plagioclase phenocrysts of latite and olivinlatite lavas range from idiomorphic to corroded and rounded shapes, and with variable degrees of kaolinization. A significant compositional variation is observed, i.e., An_{51} – An_{85} in phenocrystals and An_{54} – An_{72} in microcrysts of the groundmass (Table 2; Fig. 2). The more calcic compositions were mainly found in phenocrysts of olivinlatite lavas and in some xenoliths hosted in the latite and olivinlatite lavas. Plagioclase phenocrysts of lavas from the first period of magmatic activity at Vico volcano show higher An content (An_{75} to An_{90}).

Orthopyroxene

It occurs as euhedral phenocrysts in the ignimbrites and lava domes. It is rare in the youngest lavas, especially in the olivinlatites, where it is not abundant and commonly shows clinopyroxene exsolution lamellae. Orthopyroxene is also common in xenoliths mainly occurring in latite and olivinlatite lavas. All phenocrysts are very homogeneous and their composition lies at the boundary between enstatite and ferrosilite (Wo_{1-3}, En_{44-48}, Fs_{50-54}) (Table 3) with Mg# [$Mg/(Mg + Fe^{+2})$] ranging from 0.47 to 0.50. Orthopyroxenes from the xenoliths are identical in composition to the lava's phenocrysts.

TABLE 1 **Location and petrographic and geochemical characteristics of the studied Mti Cimini and Vico volcano samples**

SAMPLES	LOCALITY	TEXTURE							MINERALOGY		Classification	STRATIGRAPHY
		porphyritic	glomerophyric	perlitic	microlithic	vesicular	eutaxitic	fluidal	Mineral assemblage	Reverse zoned cpx		Unit
V1	Fontana Cavette	X			X				**cpx-plg**-san-bt; op-ap		trachyandesite	VICO
MP11	Fosso della Palanzana	X			X				**san-plg-bt-cpx;** op-ap		trachyandesite	VOLCANO
MP33	Fosso della Palanzana	X			X				**san-plg-bt-cpx;** op-ap		trachyandesite	
C3	quarry in La Colonneta	X				X			**ol-cpx-pl-kf-opx**; op-ap		olivinlatite	
C5	quarry in La Colonneta	X				X			**ol-cpx-pl-kf-opx**; op-ap		olivinlatite	
C6	quarry in La Colonneta	X			x				**ol-cpx-pl-kf-opx**; op-ap		olivinlatite	
C7	quarry in La Colonneta	X			x				**ol-cpx-pl-kf-opx**; op-ap		olivinlatite	OLIVINLATITIC
C8	Piangoli	X	x		x				**ol-cpx-pl-kf-opx**; op-ap	X	olivinlatite	LAVAS
C9	Coste del Cattenaccio	X			x	x			**ol-cpx-pl-kf-opx**; op-ap	X	olivinlatite	
C10	Villa Capaccini	X			X				**ol-cpx-pl-kf-opx**; op-ap	X	olivinlatite	
C11	Molinaccio	X	X		X	X			**ol-cpx-pl-kf-opx**; op-ap	x	olivinlatite	
MC1	Sasso Naticarello	X	x						**pl-kf-opx-cpx**-bt; op-ap		latite	
MC2	strada La Faggeta km 3.5	X	x						**pl-kf-opx-cpx**-bt; op		latite	
MC3	strada La Faggeta km 3.0	X	x						**pl-kf-opx-cpx**-bt; op-ap		latite	
MC4	Coste delle Macchiete	X	x		X				**pl-kf-opx-cpx**-bt; op-ap		latite	
MC5a	Sasso Naticarello	X	x						**pl-kf-opx-cpx**-bt-ol; op-ap		latite	LATITIC
MC5b	Sasso Naticarello	X	x		x				**pl-kf-opx-cpx**-bt-ol; op-ap		latite	LAVAS
MC6	Costa di Traino	X	x		X				**pl-kf-opx-cpx**-bt-ol; op-ap		latite	
MC7	Costa di Traino	X	x						**pl-kf-opx-cpx**-bt; op		latite	
MC8	Costa di Traino	X	x		X				**pl-kf-opx-cpx**-bt; op-ap		latite	
MC9	Fiannello	X	x		X				**pl-kf-opx-cpx**-bt; op		latite	
MC10	strada La Faggeta km 3.5	X	x		X				**pl-kf-opx-cpx**-bt; op-ap		latite	
MC11	Sasso Naticarello	X							**pl-kf-opx-cpx**-bt; op-ap		latite	
MP5	Mte. La Palanzana	X	x	X					**kf-bt-pl**-opx-cpx; qtz-ap-op		n.d.	
MP6	Mte. La Palanzana	X	x	x					**kf-bt-pl**-opx-cpx; qtz-ap-op		trachyandesite-trachyte	
MP7	Mte. La Palanzana	X	x	X					**kf-bt-pl**-opx-cpx; qtz-ap-op		n.d.	
MP8	Mte. La Palanzana	X	x	X		x			**kf-bt-pl**-opx-cpx; qtz-ap-op		n.d.	
MP9	Mte. La Palanzana	X	x	x					**kf-bt-pl**-opx-cpx; qtz-ap-op		trachyte	
MP10	Mte. La Palanzana	X	x	x					**kf-bt-pl**-opx-cpx; qtz-ap-op		trachyte	LAVA
MP11	Mte. La Palanzana	X			X				**kf-bt-pl**-opx-cpx; qtz-ap-op		n.d.	DOMES
MP26	Mte. La Palanzana	X		x		x			**kf-bt-pl**-opx-cpx; ap-op		n.d.	
MP27	Mte. La Palanzana	X		X					**kf-bt-pl**-opx-cpx; ap-op		n.d.	
MP30	Mte. La Palanzana	X	x						**kf-bt-pl**-opx-cpx; ap-op		n.d.	
MP33	Mte. La Palanzana	X			x	x			**kf-bt-pl**-opx-cpx; ap-op		n.d.	
MP34	Montecchio	X	x			x			**kf-bt-pl**-opx-cpx; ap-op		trachyandesite-trachyte	
MP35	Montecchio	X	x		x				**kf-bt-pl**-opx-cpx; ap-op		n.d.	
CH1	Chia						X	X	**kf-bt-pl**-opx-cpx; qtz-ap-op		n.d.	
CH2	Chia						X	x	**kf-bt-pl**-opx-cpx; qtz-ap-op		trachyte	IGNIMBRITES
CH3	Chia						X	X	**kf-bt-pl**-opx-cpx; qtz-ap-op		trachyte	
CH5	Chia						X	x	**kf-bt-pl**-opx-cpx; qtz-ap-op		n.d.	

Bold represents essential minerals.

cpx: clinopyroxene; ol: olivine; pl: plagioclase; op: opaque minerals; kf: K-feldspar; bt: biotite; ap: apatite; qtz: quartz

Small crosses refer to minor contents; n.d.: not determined.

Clinopyroxene

Clinopyroxene (Cpx) phenocrysts are very rare in the most evolved samples (dome and ignimbrite units) being more frequent in the final lavas (latites and olivinlatites units). Two types of Cpxs have been distinguished. A first type consists of euhedral to subhedral colorless-pale beige Cpxs, with homogeneous augite composition (Wo_{39-46}, En_{45-52}, Fs_{4-10}; Morimoto, 1989; Fig. 3). This Cpx is ubiquitous but it is especially abundant in the olivinlatite samples C3, C5, C6, and C7. Such samples are also characterized by Mg# [Mg/(Mg + Fe^{2+})] ranging from 0.90 to 0.99 for Cpx phenocrysts, while microlites show in general lower Mg# (0.79-0.94). A second type of Cpx is restricted to samples C8, C9, C10, and C11 of the olivinlatite unit. These Cpxs are reversely zoned phenocrysts, showing green cores and colorless rims. Cores are at the boundary between augite and diopside (Wo_{41-49}, En_{31-42}, Fs_{13-20}; Morimoto, 1989) and have Mg# varying from 0.73 to 0.82. Rims show narrower compositions (Wo_{44-46}, En_{47-50}, Fs_{5-7}), being classified as diopsides (Table 3; Fig. 3) and with Mg# similar to colorless to pale beige phenocrystals.

Petrography and composition of clinopyroxenes allow to separate olivinlatite lavas in two groups: the first characterized by the presence of pale beige augite (samples C3-C7, here after called the "O1" group; Fig. 4a) and the second by the presence of reversely zoned Cpxs (samples C8-C11, after called the "O2" group; Fig. 4b).

TABLE 2 **Selected analyses of feldspar from rocks of Mts. Cimini activity (n. d. not determined)**

	Sanidine											
Unit	Vico lavas	Vico lavas	Olivinlatitic lavas	Olivinlatitic lavas	Olivinlatitic lavas	Olivinlatitic lavas	Latitic lavas	Latitic lavas	Lava domes	Lava domes	Ignimbrite	Ignimbrite
Sample	V1	V1	C8	C9	C6	C7	MC6	MC6	MP10	MP6	CH3	CH3
SiO_2	64.2	65.04	64.44	64.07	63.46	64.37	65.53	65.32	65.21	65.84	65.66	66.28
TiO_2	0.05	0.16	0.04	–	0.02	–	0.03	0.05	0.05	0.03	0.01	0.04
Al_2O_3	19.58	19.41	18.67	18.60	18.40	18.09	18.94	18.90	18.78	18.78	18.88	18.72
Fe_2O_3	0.28	0.21	0.09	0.11	0.00	0.03	0.00	0.05	0.05	0.00	0.02	0.03
MgO	0.02	0.028	–	–	–	–	–	–	–	–	–	–
CaO	0.81	0.74	0.29	0.27	0.28	0.18	0.26	0.28	0.21	0.19	0.25	0.23
BaO	n.d	n.d	0.70	0.48	0.72	0.45	n.d	n.d	n.d	n.d	0.34	n.d
Na_2O	2.41	3.012	2.12	1.94	1.53	1.51	2.06	2.24	2.65	1.84	1.99	2.07
K_2O	11.77	11.46	13.08	13.39	14.06	13.80	13.08	12.87	12.10	13.15	13.09	13.16
Sum Ox%	99.11	100.08	99.44	98.87	98.46	98.43	99.89	99.78	99.05	99.86	100.29	99.52
Si	2.951	2.958	2.979	2.979	2.977	3.004	2.990	2.990	2.990	3.004	2.994	2.995
Ti	0.002	0.006	0.001	0.000	0.001	0.000	0.000	0.002	0.002	0.001	0.000	0.001
Al/Al^{IV}	1.061	1.040	1.017	1.019	1.017	0.995	1.020	1.019	1.016	1.010	1.015	1.012
Fe^{3+}	0.011	0.008	0.003	0.004	0.000	0.001	0.000	0.002	0.002	0.000	0.001	0.001
Mg	0.001	0.002	–	–	–	–	–	–	–	–	–	–
Ca	0.040	0.036	0.014	0.013	0.014	0.009	0.010	0.014	0.147	0.009	0.012	0.011
Ba	0.000	0.000	0.013	0.009	0.013	0.008	0.000	0.000	0.000	0.000	0.006	0.000
Na	0.215	0.266	0.190	0.175	0.139	0.137	0.180	0.199	0.235	0.163	0.176	0.184
K	0.690	0.666	0.772	0.794	0.842	0.822	0.760	0.751	0.709	0.765	0.762	0.770
Sum Cat#	4.970	4.981	4.990	4.994	5.003	4.977	4.970	4.980	4.969	4.954	4.967	4.975
Ab	22.74	27.46	19.19	17.65	13.81	14.00	19.09	20.60	24.65	17.40	18.45	19.04
An	4.21	3.73	1.45	1.35	1.38	0.94	1.34	1.44	1.06	0.98	1.28	1.18
Or	73.05	68.81	83.50	84.22	70.60	79.30	79.57	77.96	74.30	81.62	79.64	79.78

	Plagioclase									
Unit	Olivinlatitic lavas	Olivinlatitic lavas	Olivinlatitic lavas	Olivinlatitic lavas	Latitic lavas	Latitic lavas	Lava domes	Lava domes	Ignimbrite	Ignimbrite
Sample	C8	C8	C6	C6	MC6	MC6	MP10	MP6	CH3	CH3
SiO_2	54.64	47.76	54.46	48.08	54.88	55.51	53.43	54.91	54.74	50.36
TiO_2	0.01	0.03	0.00	0.00	0.01	0.04	0.00	0.02	0.02	0.05
Al_2O_3	28.12	31.78	29.02	33.70	28.75	28.64	29.09	28.60	28.47	31.28
Fe_2O_3	0.19	0.71	0.13	0.22	0.21	0.20	0.26	0.18	0.20	0.15
MgO	0.03	0.12	0.01	0.03	0.00	0.01	0.03	0.01	0.03	0.03
CaO	10.62	15.83	11.04	15.82	11.23	10.91	11.61	11.29	11.23	14.62
Na_2O	5.06	2.30	4.62	1.97	4.66	4.73	4.70	4.59	4.89	3.25
K_2O	0.56	0.35	0.59	0.17	0.61	0.63	0.52	0.58	0.54	0.28
Sum Ox%	99.23	98.90	99.87	99.99	100.34	100.69	99.70	100.19	100.13	100.02
Si	2.485	2.219	2.460	2.200	2.470	2.487	2.430	2.474	2.472	2.299
Ti	0.000	0.001	0.000	0.000	0.000	0.001	0.000	0.001	0.001	0.002
Al/Al^{IV}	1.507	1.741	1.560	1.816	1.525	1.512	1.559	1.519	1.515	1.683
Fe^{3+}	0.006	0.025	0.005	0.009	0.008	0.007	0.010	0.007	0.007	0.006
Mg	0.002	0.009	0.001	0.002	0.000	0.001	0.002	0.001	0.002	0.002
Ca	0.518	0.788	0.535	0.775	0.542	0.524	0.566	0.545	0.543	0.715
Na	0.446	0.207	0.405	0.175	0.406	0.411	0.414	0.401	0.428	0.288
K	0.033	0.021	0.034	0.010	0.035	0.036	0.030	0.033	0.031	0.016
Sum Cat#	4.998	5.011	4.986	4.985	4.987	4.980	5.013	4.982	4.999	5.010
Ab	44.79	20.37	41.61	18.21	41.34	42.33	41.00	40.96	42.72	28.25
An	51.93	77.58	54.92	80.79	55.10	53.96	55.98	55.64	54.19	70.17
Or	2.29	0.89	0.82	0.56	3.40	3.25	3.22	3.77	1.88	1.75

All Fe as Fe_2O_3

Clinopyroxene occurs as euhedral to subhedral pale green phenocrysts on samples from Vico. They are very homogeneous diopside (Wo_{46-49}, En_{38-39}, and Fs_{14-16}) and Mg# in the range 0.76 – 0.84. These results are similar to the values obtained for cores of the reverse zoned Cpxs of the O2 olivinlatite lavas of Mts. Cimini. Moreover, they overlap data of Perini et al. (2000) and Perini and Conticelli (2002) for the Vico volcanic products (see also Cellai et al., 1994).

Titanium and aluminum contents were used by Conticelli (1998) to discriminate among Cpxs crystallized from potassic magmas with different petrological affinity. On this basis, Cpxs are classified as Lamproite, Transitional or Roman-Type clinopyroxenes (Fig. 5). Mts. Cimini Cpxs show a widespread distribution, occurring in all fields (Fig. 5). Cpxs which plot in the Roman-type field mainly correspond to the cores of the reverse zoned clinopyroxenes of O2 olivinlatites, and plot in the same area as Vico clinopyroxenes. In contrast, clinopyroxenes of the O1 olivinlatites mostly plot in the Lamproite field.

Olivine

It only presents in the latite and olivinlatite lavas. It is subehedral with a maximum sizes of 1 mm. Some olivines show rims altered to iddingsite. Moreover, in some olivinlatite lavas (especially those belonging to the

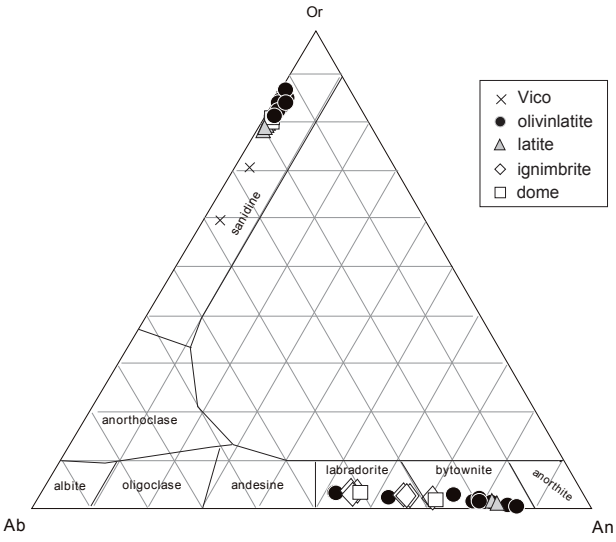

FIGURE 2 | **Classification of feldspars using the triangular diagram Or-Ab-An (Deer et al. 1963).**

O2 group), the largest olivine phenocrysts commonly show skeletal morphologies. The chemical composition of olivines is very homogeneous with Fo_{89-93} (Table 4). No significant compositional variations were detected between phenocrysts and microphenocrysts.

Biotite

Biotite phenocrysts are frequent in domes and ignimbrite, and very rare in the final lavas (especially in the olivinlatite lavas). They occur as euhedral phenocrysts with Mg# within the range 0.50 – 0.75 (Table 5). These compositions are similar to those observed in biotites from Vico volcano (e.g., Perini et al., 2000; Perini and Conticelli, 2002).

WHOLE-ROCK GEOCHEMISTRY

Major and trace element data

Similarly to most of subduction-related volcanic suites (Keller, 1983; Thorpe et al., 1984; Hickey et al., 1986), Mts. Cimini magmas are characterized by highly variable Al_2O_3 and CaO, low TiO_2, Na_2O, and MgO with respect to their silica content (~55 - 75 wt.%; Table 6 and Fig. 6). These rocks are classified as latites, trachyandesites, and trachytes, according to the T.A.S. diagram (Le Maitre et al., 2002; Fig. 6h), and are characterized by relatively high K_2O/Na_2O values (> 1.7 for MgO > 3 wt.%). Silica content progressively decreases with the age of Mts. Cimini magmatic products.

MgO, CaO, P_2O_5, and partially TiO_2, progressively decrease with the increase of SiO_2 as has been found for the Vico volcano. This can be interpreted as olivine + clinopyroxene + apatite removal during magma fractionation (Fig. 6a, f). Clinopyroxene segregation is also indicated by the negative correlation of CaO/Al_2O_3 ratios with SiO_2 (Fig. 6g).

Mts. Cimini rocks do not display significant variation in K_2O with increasing SiO_2 content, whereas those from Vico record a significant K-enrichment (Fig. 6d). Buffering of K_2O content with increasing silica, coupled with Na_2O enrichment, could imply significant K-rich mineral fractionation (e.g., sanidine and biotite). Magmas with MgO > 5% wt (mostly olivinlatites) are heterogeneous in TiO_2 and P_2O_5, with two different enrichment levels at comparable SiO_2 content (Fig. 6a-f). The P-Ti-rich olivinlatites belong to the O1 group and appear as the most primitive products (highest MgO content) on a trend of magma differentiation involving the whole Mts. Cimini magmas. In contrast, the Ti-P-poor olivinlatites (belonging to the O2 group) show similarities with the nearby Vico volcano trachybasalts, thus plotting on a different trend of magma evolution identified by the Mts. Cimini magmas (Fig. 6a, f).

Ni (Fig. 7a) and Co (not shown) display positive trends with MgO, supporting significant fractionation of olivine during the evolution of these lavas. In contrast, a slope change in the liquid line evolution path from olivinlatites to latites suggests the beginning of clinopyroxene crystallization. The Mg-Ni rich samples are also enriched in Zr and partly Nb (High Field Strength Elements or HFSE), but not Y, which shows slightly homogeneous compositions with respect to MgO variation (Fig. 7b-d). Low Field Strength Elements (LFSE) composition is about constant for the whole data collection. The olivinlatitic samples are characterized by a

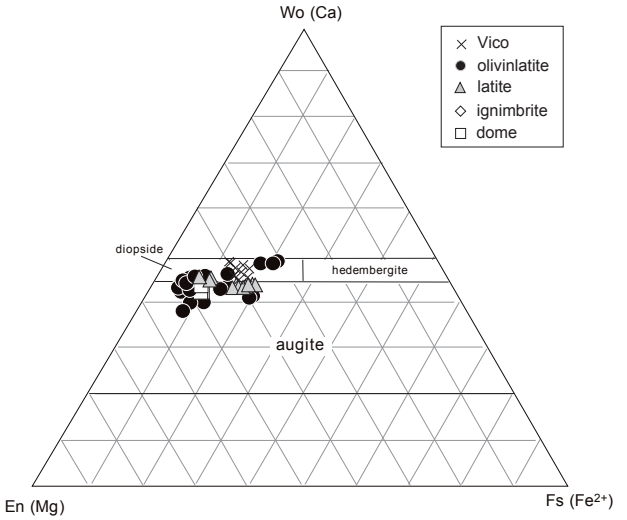

FIGURE 3 | **Classification of clinopyroxenes (Cpx) using the triangular diagram Wo-En-Fs of Morimoto (1989).**

TABLE 3 | **Selected analyses of pyroxenes from rocks of Mts. Cimini activity**

Orthopyroxenes

Unit	Olivinlatitic lavas	Olivinlatitic lavas	Olivinlatitic lavas	Olivinlatitic lavas	Latitic lavas	Latitic lavas	Lava domes	Lava domes	Ignimbrite	Ignimbrite
Sample	C8	C8	C6	C6	MC5b	MC6	MP10	MP10	CH3	CH3
SiO_2	50.27	50.25	50.17	49.07	51.68	51.74	50.17	49.48	51.53	51.70
TiO_2	0.25	0.14	0.13	0.14	0.19	0.15	0.13	0.19	0.15	0.16
Al_2O_3	0.49	0.62	0.31	0.45	0.29	0.31	0.43	0.46	0.29	0.27
FeOt	30.43	30.73	30.96	30.16	29.64	29.35	31.57	32.01	29.60	30.16
MnO	0.80	0.78	0.97	0.81	0.82	0.75	0.77	0.92	0.80	0.79
MgO	16.15	16.06	16.26	15.90	16.34	15.84	15.40	15.43	16.18	16.11
CaO	1.20	0.72	0.99	1.24	1.21	1.16	1.11	0.76	1.33	1.19
Na_2O	0.04	0.03	–	0.01	–	0.05	–	–	0.02	0.01
Cr_2O_3	0.04	0.03	0.03	–	–	–	–	–	–	–
Sum Ox%	99.67	99.36	99.82	97.78	100.17	99.35	99.59	99.25	99.90	100.39
Si	1.959	1.966	1.955	1.950	1.997	2.011	1.970	1.950	1.990	1.990
Ti	0.007	0.004	0.004	0.004	0.006	0.005	0.004	0.006	0.045	0.005
Al/Al^{IV}	0.023	0.028	0.014	0.021	0.013	0.014	0.020	0.021	0.013	0.013
Cr2O3	0.001	0.001	0.001	0.000	0.000	0.000	0.000	0.000	0.000	0.000
Fe^{3+}	0.045	0.032	0.068	0.071	0.000	0.000	0.037	0.071	0.000	0.000
Fe^{2+}	0.947	0.973	0.941	0.931	0.958	0.954	0.999	0.984	0.960	0.974
Mn	0.026	0.026	0.032	0.027	0.027	0.025	0.026	0.031	0.026	0.026
MgO	0.938	0.937	0.944	0.942	0.941	0.918	0.900	0.906	0.935	0.928
Ca	0.050	0.030	0.041	0.053	0.050	0.049	0.047	0.032	0.055	0.026
Na	0.003	0.002	0.000	0.000	0.001	0.004	0.000	0.000	0.002	0.001
Sum Cat #	4.000	4.000	4.000	4.000	3.992	3.980	4.000	4.000	3.992	3.993
Wo	2.50	1.51	2.04	2.61	2.54	2.48	2.32	1.59	2.80	2.49
En	46.75	46.87	46.60	46.53	47.63	47.19	44.83	44.78	47.31	46.92
Fs	50.75	51.62	51.36	50.87	49.83	50.33	52.85	53.64	49.89	50.59
#Mg	0.50	0.49	0.50	0.50	0.49	0.50	0.48	0.47	0.49	0.49

Clinopyroxenes

Unit	Vico lavas	Vico lavas	Olivinlatitic lavas	Olivinlatitic lavas	Olivinlatitic lavas	Olivinlatitic lavas	Olivinlatitic lavas	Latitic lavas	Latitic lavas	Latitic lavas	Latitic lavas	Ignimbrite
Sample	V1	V1	C8	C8	C8	C9	C9	MC6	MC6	MC5b	MC5b	CH3
Where	phenocryst	phenocryst	rim	core	microcryst	rim	core	microcryst	phenocryst	microcryst	microcryst	microcryst
SiO_2	50.86	49.37	52.08	50.33	51.06	51.50	47.82	49.22	51.93	47.81	52.09	52.82
TiO_2	0.65	0.79	0.33	0.34	0.58	0.47	0.60	1.12	0.58	1.80	0.98	0.21
Al_2O_3	3.32	4.82	2.77	2.31	3.41	2.19	3.80	4.51	2.05	7.02	3.78	0.55
Cr_2O_3	–	–	0.86	0.04	0.19	0.57	0.06	–	–	–	–	–
Fe_2O_3	2.17	3.51	0.88	2.56	2.83	2.09	6.33	3.79	0.15	2.46	0.99	0.00
FeO	6.99	5.51	2.60	8.95	2.14	1.37	4.49	2.57	5.80	6.19	3.29	13.87
MnO	0.30	0.25	0.14	0.46	0.14	0.06	0.20	0.17	0.16	0.22	0.16	0.46
MgO	13.23	12.92	16.92	13.31	16.56	17.41	11.42	15.83	15.92	13.22	16.95	11.76
CaO	22.48	22.97	22.30	20.00	22.60	22.23	22.88	21.81	21.47	21.50	22.29	20.79
Na_2O	0.36	0.33	0.23	0.37	0.18	0.22	0.72	0.21	0.16	0.26	0.21	0.09
Sum Ox%	100.38	100.45	99.12	98.68	99.69	98.11	98.32	99.22	98.21	100.50	100.80	100.55
Si	1.8920	1.8352	1.9150	1.9150	1.8750	1.9100	1.8320	1.8200	1.9425	1.7700	1.8900	1.9956
Ti	0.0181	0.0220	0.0090	0.0100	0.0160	0.0130	0.0170	0.0300	0.0162	0.0500	0.0300	0.0059
Al/Al^{IV}	0.1458	0.2112	0.0850	0.0850	0.1250	0.0900	0.1680	0.1900	0.0904	0.3100	0.1600	0.0245
Al_{VI}	0.0000	0.0000	0.0350	0.0190	0.0220	0.0060	0.0030	0.0000	0.0000	0.0000	0.0000	0.0000
Cr	0.0000	0.0000	0.0250	0.0010	0.0050	0.0170	0.0020	0.0000	0.0000	0.0000	0.0000	0.0000
Fe^{3+}	0.0607	0.0981	0.0240	0.0730	0.0780	0.0580	0.1830	0.0800	0.0042	0.0685	0.0270	0.0000
Fe^{2+}	0.2173	0.1712	0.0800	0.2850	0.0660	0.0430	0.1440	0.0800	0.1814	0.1919	0.0997	0.4383
Mn	0.0096	0.0078	0.0040	0.0150	0.0050	0.0020	0.0060	0.0100	0.0050	0.0069	0.0050	0.0146
Mg	0.7338	0.7158	0.9270	0.7550	0.9060	0.9620	0.6520	0.8700	0.8874	0.7302	0.9145	0.6622
Ca	0.8959	0.9150	0.8780	0.8150	0.8890	0.8830	0.9390	0.8700	0.8606	0.8538	0.8650	0.8417
Na	0.0262	0.0234	0.0160	0.0270	0.0130	0.0150	0.0530	0.0200	0.0121	0.0189	0.0144	0.0068
Sum Cat#	4.0000	4.0000	4.0000	4.0000	4.0000	4.0000	4.0000	4.0000	4.0000	4.0000	4.0000	4.0000
Wo(Ca)	46.73	47.95	45.89	41.96	45.74	45.34	48.81	44.84	44.39	46.11	45.25	43.01
En(Mg)	38.26	37.52	48.44	38.85	46.63	49.39	33.89	45.28	45.78	39.45	47.87	33.84
Fs(Fe2+)	15.01	14.53	5.68	19.19	7.63	5.27	17.30	9.87	9.83	14.44	6.88	23.14
Mg#	0.77	0.81	0.92	0.73	0.93	0.96	0.82	0.92	0.83	0.79	0.90	0.60

Fe^{2+} and Fe^{3+} were calculated using the XMAS V.8.2 software from SAMX (France) and following the indications of Droop (1987)

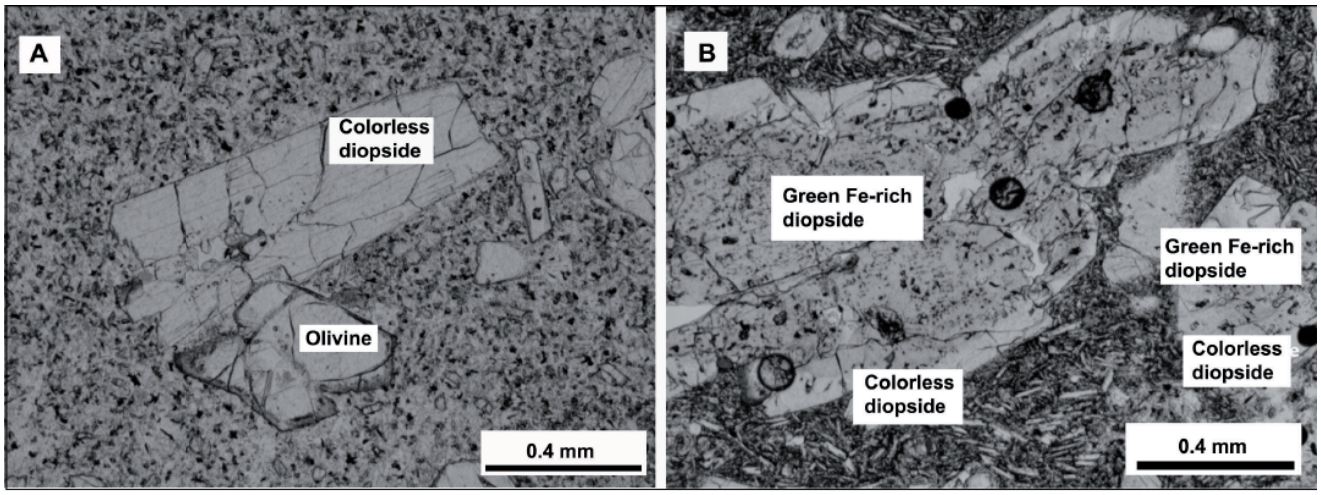

FIGURE 4 | **Microphotographs: A) colorless clinopyroxene (diopside) phenocryst and partially iddiginsitized olivine, surrounded by a matrix formed by microcrystals of clinopyroxenes and oxides in O1-type olivinlatite (sample C6); B) reverse zoned clinopyroxenes with salitic cores and diopsidic rims in O2-type olivinlatite (sample C8). These phenocrystals are surrounded by a microlitic matrix consisting of clinopyroxene microcrystals of diopsidic composition, and oxides.**

larger range of trace element contents, both in the HFSE and LFSE, grouping into O1 and O2 olivinlatites, with distinct composition (Fig. 7).

Mts. Cimini magmas show variable highly incompatible element ratios, which are positively correlated with MgO and TiO_2 (e.g., Fig. 8). Such variability is similar to that of Vico (Fig. 8) and most of the RMP magmas. At Mts. Cimini the largest scatter in highly incompatible element ratios is recorded among olivinlatite samples.

Most of the Mts. Cimini samples show similar, slightly concave REE patterns, with variable enrichment in LREE [$(Ce/Yb)_n$-normalized to CI chondrite value- between 16 and 72] and ubiquitous Eu-negative anomaly (Fig. 9a). Fractionation is stronger for MREE and HREE, especially for the O2 olivinlatites (insert in Fig. 9b), suggesting residual amphibole and/or titanite in their mantle source.

Primordial mantle-normalized bulk rock trace element abundances of the Mts. Cimini volcanics show comparable patterns, with notable enrichment of the most incompatible elements (from P to Rb, with some exceptions) from ten to one thousand times the primordial mantle abundances (Fig. 9b). Multi-element spiderdiagram are characterized by negative anomalies of Ba, Nb, P and Ti, and peaks of Rb, Th (U), and Pb, thus resembling those of subduction-related volcanic rocks (Thorpe et al., 1984; Hickey et al., 1986).

Sr, Nd and Pb isotope data

As a whole, Mts. Cimini volcanics have Sr, Nd and Pb isotope compositions that are typical of crust-derived material (e.g., Hofmann, 1997). They show the most radiogenic $^{87}Sr/^{86}Sr$ and the lowest $^{143}Nd/^{144}Nd$ ratios among both the RMP and TMP, overlapping the field of circum-Mediterranean granites (Juteau et al., 1986). Their Pb isotope compositions plot above the Northern Hemisphere Reference Line (NHRL), within the field of pelagic sediments (Ben Othman et al., 1989). Mts. Cimini samples display narrow ranges in $^{143}Nd/^{144}Nd$ (0.51205-0.51214), $^{206}Pb/^{204}Pb$ (18.705-18.726), $^{207}Pb/^{204}Pb$ (15.665-15.687), and $^{208}Pb/^{204}Pb$ (38.937-39.019) ratios (Table 7, Fig. 10). In contrast, they show a wider range in $^{87}Sr/^{86}Sr$ ratios (0.71218-0.71568), with the maximum variability recorded by the olivinlatites. O1 type is characterized by the highest $^{87}Sr/^{86}Sr$ ratios (>0.71523), whereas O2 type shows the lowest values of Sr-isotopes (<0.71348). The increase of $^{87}Sr/^{86}Sr$ ratios correlates negatively to Sr variation (Fig. 10e).

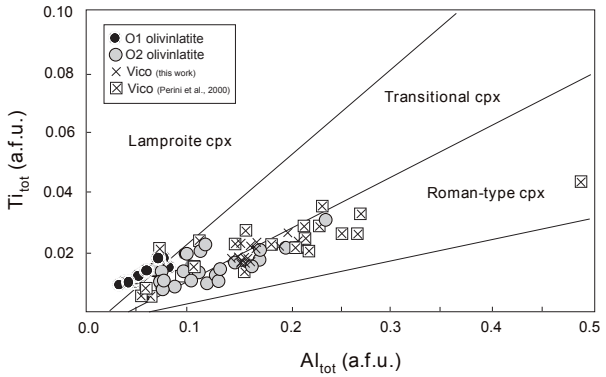

FIGURE 5 | **Al vs. Ti variation diagram for the clinopyroxenes from the olivinlatite unit of Mts. Cimini, as well as from the rocks of Vico volcano (this work and Perini et al., 2000). Fields for clinopyroxene from Italian rocks are from Conticelli (1998).**

TABLE 4 | **Selected analyses of olivines from rocks of Mts. Cimini activity**

Unit	Olivinlatitic lavas										
Sample	C8	C8	C8	C9	C9	C9	C9	C6	C6	C6	C7
SiO_2	40.56	40.43	39.63	40.83	40.11	40.51	39.55	40.31	39.81	40.30	39.77
TiO_2	0.01	0.02	0.01	-	0.02	-	0.01	-	0.01	0.01	0.04
Al_2O_3	0.01	0.04	-	0.02	0.04	0.01	0.01	0.02	0.03	-	-
FeO	10.34	10.15	11.01	8.51	9.29	7.80	14.20	6.91	6.48	6.77	10.61
MnO	0.21	0.11	0.17	0.17	0.18	0.10	0.26	0.03	0.09	0.06	0.09
MgO	48.57	48.61	48.52	48.99	50.03	50.44	45.16	51.35	52.40	51.16	48.47
CaO	0.25	0.22	0.21	0.24	0.25	0.24	0.24	0.18	0.18	0.17	0.24
Cr_2O_3	0.03	0.05	0.07	0.06	0.08	0.09	0.11	0.09	0.16	0.07	0.09
NiO	0.32	0.27	0.22	0.37	0.29	0.43	0.22	0.40	0.65	0.44	0.32
Sum Ox%	100.30	99.89	99.84	99.19	100.28	99.62	99.76	99.29	99.81	98.98	99.63
Si	0.996	0.995	0.982	1.004	0.982	0.991	0.994	0.985	0.970	0.988	0.986
Ti	0.000	0.000	0.000	0.000	0.000	0.000	0.000	0.000	0.000	0.000	0.001
Al	0.000	0.001	0.000	0.001	0.001	0.000	0.000	0.001	0.001	0.000	0.000
Cr	0.001	0.001	0.001	0.001	0.002	0.002	0.002	0.002	0.003	0.001	0.002
Fe^{2+}	0.212	0.209	0.228	0.175	0.190	0.159	0.299	0.141	0.132	0.139	0.220
Mn	0.004	0.002	0.004	0.003	0.004	0.002	0.006	0.001	0.002	0.001	0.002
Mg	1.777	1.783	1.792	1.796	1.825	1.839	1.692	1.871	1.903	1.869	1.790
Ca	0.006	0.006	0.006	0.006	0.007	0.006	0.007	0.005	0.005	0.005	0.006
Ni	0.006	0.005	0.004	0.007	0.006	0.009	0.004	0.008	0.013	0.009	0.006
Sum Cat#	3.004	3.003	3.017	2.995	3.016	3.008	3.004	3.013	3.028	3.012	3.013
Fo	89.3	89.5	88.7	91.1	90.6	92	85	93	93.5	93.1	89.1

TABLE 5 | **Selected analyses of mica from rocks of Mts. Cimini activity**

Unit	Lava domes					
Sample	MP6	MP6	MP9	MP9	MP10	MP10
SiO_2	37.02	36.79	35.73	36.41	34.90	34.77
TiO_2	5.26	3.94	6.57	6.35	6.30	6.81
Al_2O_3	14.96	16.32	13.72	14.19	13.70	14.42
MgO	11.39	17.24	10.80	10.89	10.49	10.76
CaO	0.02	0.02	0.04	0.00	0.02	0.04
MnO	0.10	0.15	0.15	0.07	1.07	0.02
FeO	17.93	11.41	19.18	18.82	19.41	20.24
Na_2O	0.44	0.43	0.42	0.36	0.29	0.32
K_2O	8.82	9.00	8.84	8.84	8.98	8.88
H_2O*	3.99	4.09	3.92	3.97	3.88	3.93
Sum Ox%	99.95	99.41	99.36	99.89	99.00	100.19
Si	5.557	5.400	5.461	5.507	5.400	5.30
Ti	0.594	0.435	0.755	0.722	0.730	0.78
Al	2.649	2.823	2.472	2.529	2.490	2.59
Mg	2.549	3.771	2.459	2.456	2.419	2.45
Ca	0.004	0.004	0.006	0.000	0.003	0.01
Mn	0.012	0.018	0.002	0.009	0.141	0.002
Fe	2.251	1.401	2.452	2.380	2.511	2.581
Na	0.127	0.123	0.123	0.105	0.087	0.094
K	1.689	1.686	1.723	1.705	1.771	1.728
Sum Cat#	15.432	15.659	15.473	15.415	15.553	15.531

* H_2O was calculated using the program Formula 1 from the XMAS V.8.2 software (SAMX, France) and following the indications of Deer et al. (1992). 4 OH in the hydrous mineral formula were considered for 22 oxygen atoms.

DISCUSSION

Geochemical data on Mts. Cimini volcanism show negative correlations of most major elements with SiO_2, thus suggesting that magmatic history was dominated by processes occurred at shallow level, e.g., in crustal magmatic reservoirs. Magma evolution through fractional crystallization (plagioclase ± sanidine, pyroxene, biotite, olivine and oxide separation), in some cases associated with assimilation of local continental crust (Conticelli et al., 1992, 2002), mostly characterized the progression of latites, dome lavas and ignimbrites (Figs. 6 and 7). As supported by simple mass balance calculation (Stormer and Nicholls, 1978), evolution by fractional crystallization of the above mentioned mineral phases could fit the major element composition of latites and dome lavas from O1 olivinlatites.

TABLE 6 | **Whole-rock major (wt.% oxides) and trace (ppm) element abundance for the volcanic rocks of Mts. Cimini and Vico. Mg# is calculated as [Mg/(Mg + Fe^{+2})]**

Unit	Vico	Vico	Vico	olivinlatite	olivinlatite	olivinlatite	olivinlatite	olivinlatite	olivinlatite	olivinlatite	olivinlatite	latite	latite	latite	latite
Sample	MP33a	MP11	V1	C3	C5	C6	C7	C8	C9	C10	C11	MC8	MC9a	MC9b	MC10
wt%															
SiO_2	59.84	59.25	56.33	54.30	57.65	57.31	55.99	55.37	55.78	54.41	54.83	59.61	59.86	59.77	57.64
TiO_2	0.72	0.60	0.77	1.31	1.14	1.28	1.16	0.75	0.88	0.87	0.94	0.88	0.99	1.06	0.95
Al_2O_3	20.77	19.89	17.59	16.53	14.23	13.96	14.57	16.64	14.68	15.44	14.02	15.61	15.68	15.46	15.20
Fe_2O_3t	3.76	3.65	6.09	6.99	5.59	5.51	6.04	5.89	5.73	5.83	5.66	5.56	5.25	5.49	5.49
MnO	0.15	0.15	0.10	0.10	0.08	0.07	0.09	0.10	0.09	0.09	0.09	0.08	0.08	0.08	0.08
MgO	0.72	0.79	2.87	8.51	7.44	7.31	8.02	5.21	6.36	6.37	6.65	4.15	4.16	4.13	5.73
CaO	1.85	2.90	6.28	5.15	6.65	6.71	6.46	7.22	6.85	6.81	6.61	5.91	5.78	5.58	6.72
Na_2O	2.89	3.60	2.45	0.91	1.39	1.49	1.32	2.09	1.69	1.59	1.51	2.11	2.18	2.00	2.08
K_2O	9.11	9.00	7.07	5.71	5.93	5.97	5.97	4.34	5.27	5.15	5.92	5.63	5.74	5.79	5.23
P_2O_5	0.20	0.19	0.48	0.49	0.44	0.41	0.45	0.26	0.32	0.32	0.38	0.45	0.39	0.41	0.41
LOI	2.34	1.56	0.98	3.20	0.60	1.19	1.01	0.27	0.14	2.74	2.13	0.60	0.85	1.20	0.37
Mg#	0.30	0.33	0.51	0.73	0.75	0.75	0.75	0.67	0.71	0.71	0.73	0.63	0.64	0.63	0.70
ppm															
Ba	357	256	1166	852	712	728	708	911	1086	1166	1181	901	936	1005	1063
Co	4.0	3.0	16.0	31.3	27.0	23.4	23.5	32.2	36.4	28.8	34.9	20.3	18.2	19.7	23.6
Cr	26.0	38.0	37.0	325	307	302	236	139	279	228	285	106	108	133	210
Cu	0.0	1.0	22.0	42.7	29.6	28.7	29.9	28.1	60.5	35.1	36.1	28.7	23.9	27.0	41.4
Ga	21.0	21.0	20.0	22.4	19.6	20.7	21.6	21.9	20.6	21.5	20.6	19.2	20.4	20.6	20.1
Nb	58.0	58.0	19.0	25.3	21.2	20.4	21.2	17.8	21.5	21.4	22.6	16.5	16.6	19.1	16.6
Ni	0.0	1.0	9.0	208	173	160	166	60.2	140	120	161	49.0	43.8	46.2	97.1
Pb	190.0	179.0	94.0	46.1	41.7	38.9	41.0	71.6	62.6	66.5	75.5	62.5	66.0	65.9	63.9
Rb	307	596	396	268	401	403	341	186	349	275	353	328	343	360	331
Sn	7.00	9.00	3.00	8.70	5.60	4.70	6.70	6.80	5.80	6.10	9.50	7.80	8.60	7.70	5.80
Sr	470	595	1191	355	409	416	451	623	646	659	747	545	548	556	623
Th	251	251	83.0	59.7	50.9	53.9	51.9	39.0	50.7	51.2	67.0	46.3	48.0	52.7	46.2
U	-	-		10.5	10.8	10.7	10.0	-	-	-	-	-	-	-	-
V	40.0	87.0	111	104	95.4	95.5	86.8	106	103	103	105	92.4	57.8	93.1	98.7
Y	86.0	63.0	38.0	32.4	24.7	24.3	23.9	27.0	26.0	26.3	26.1	27.3	25.0	32.2	28.3
Zn	74.0	70.0	65.0	85.4	72.2	68.3	70.8	68.4	64.6	63.6	69.5	64.4	63.0	67.6	64.2
Zr	1055	1064	398	530	462	459	462	216	348	335	380	306	310	334	341
Hf	-	-	-	15.36	5.23	8.06	6.64	5.07	8.84	7.95	9.88	-	-	-	-
La	349	240	121	110	83.9	85.7	86.4	68.7	84.0	85.5	105	113	96.1	121	131
Ce	500	408	205	214	188	189	189	132	168	178	217	223	195	205	249
Pr	61.0	41.8	26.5	30.5	24.4	25.5	24.5	7.30	9.86	9.92	12.7	25.7	22.3	26.5	30
Nd	206	137	103	123	95.9	101	98.9	56.1	78.9	79.2	103	99.9	86.5	103	117
Sm	29.6	19.5	16.1	18.0	14.5	14.7	14.9	4.43	5.79	5.83	7.60	15.6	13.6	16.1	17.9
Eu	3.65	2.35	2.65	2.97	2.31	2.44	2.44	0.87	1.02	1.00	1.30	2.65	2.30	2.65	3.05
Gd	25.1	16.5	11.7	14.5	11.2	11.8	11.3	3.79	4.44	4.49	5.63	11.6	9.8	11.7	13.2
Tb	3.2	1.95	1.40	1.48	1.17	1.15	1.19	0.44	0.48	0.48	0.58	1.40	1.20	1.40	1.55
Dy	14.4	9.10	6.25	7.56	6.09	6.22	6.18	2.14	2.11	2.15	2.42	6.20	5.25	6.25	6.80
Ho	2.75	1.65	1.05	1.02	0.80	0.82	0.84	0.39	0.35	0.36	0.39	1.10	0.90	1.05	1.20
Er	8.05	4.90	2.95	3.12	2.50	2.62	2.52	1.07	0.99	0.99	1.05	3.00	2.50	2.95	3.25
Tm	1.10	0.55	0.40	0.34	0.26	0.28	0.30	0.14	0.13	0.13	0.13	0.40	0.35	0.40	0.40
Yb	7.45	4.90	2.50	2.48	1.91	1.95	1.92	0.88	0.83	0.82	0.84	2.50	2.10	2.50	2.70
Lu	1.15	0.8	0.4	0.34	0.29	0.27	0.29	0.13	0.12	0.12	0.12	0.34	0.35	0.35	0.55

Unit	latite	latite	latite	latite	latite	latite	latite	latite	latite	dome	dome	dome	dome	dome	ignimbrite	ignimbrite
Sample	MC11	MC1	MC2	MC3	MC4	MC5a	MC5b	MC6	MC7	MP10	C1	MP34	MP6	MP9	CH2	CH5
wt%																
SiO_2	55.93	59.78	60.47	59.34	59.71	58.30	59.56	59.41	59.83	64.81	75.55	61.82	62.96	64.00	63.14	63.14
TiO_2	1.12	1.05	0.88	0.97	1.01	0.99	0.91	0.87	1.01	0.78	1.02	1.01	0.95	0.91	0.73	0.67
Al_2O_3	15.99	16.22	15.64	16.25	15.69	17.47	16.14	15.45	15.77	16.42	9.70	18.26	16.99	16.53	16.60	16.68
Fe_2O_3t	6.29	5.83	5.19	5.80	5.37	6.04	5.40	5.34	5.25	4.84	5.68	5.40	4.73	4.48	4.51	4.52
MnO	0.10	0.08	0.08	0.08	0.07	0.10	0.09	0.08	0.08	0.09	0.05	0.08	0.07	0.07	0.07	0.07
MgO	5.33	4.30	3.78	4.19	4.19	4.24	3.93	4.63	4.12	1.76	0.76	2.20	2.01	1.89	2.18	2.25
CaO	7.35	4.69	5.75	5.38	5.77	5.34	6.06	6.01	5.62	3.06	0.45	3.57	3.79	3.70	4.14	4.28
Na_2O	1.87	1.64	2.22	1.79	1.99	1.63	2.24	2.12	2.02	2.37	1.19	2.31	2.77	2.72	2.63	2.54
K_2O	5.50	6.00	5.60	5.81	5.81	5.41	5.29	5.63	5.89	5.33	5.28	4.98	5.41	5.42	5.62	5.47
P_2O_5	0.52	0.44	0.42	0.42	0.40	0.50	0.37	0.45	0.39	0.36	0.38	0.35	0.32	0.30	0.37	0.40
LOI	1.33	2.08	1.28	2.79	1.06	2.93	0.33	0.23	0.82	1.33	3.55	1.67	1.44	2.01	1.25	1.25
Mg#	0.66	0.62	0.62	0.62	0.64	0.61	0.62	0.66	0.64	0.45	0.23	0.48	0.49	0.49	0.52	0.53
ppm																
Ba	944	1013	824	1040	1040	946	827	941	1097	770	1186	924	974	862	1076	923
Co	25.7	19.9	18.7	19.1	19.1	21.6	16.7	20.5	18.1	11.9	8.4	13.0	11.0	11.3	10.8	9.4
Cr	92.1	108	72.1	103	103	72.2	62.4	105	107	71.7	45.1	71.0	76.8	70.8	80.3	78.8
Cu	28.7	28.5	24.5	27.6	27.6	30.1	20.9	25.4	24.2	27.7	6.3	7.6	10.0	12.4	10.2	3.7
Ga	21.3	21.4	20.4	21.3	21.3	22.0	21.0	21.2	20.8	22.0	16.4	24.1	22.3	21.3	21.1	21.2
Nb	16.1	18.8	16.5	17.5	17.5	18.1	16.2	16.5	16.2	17.7	20.7	17.9	16.1	16.3	14.8	15.1
Ni	57.5	54.0	40.8	48.9	48.9	44.5	37.3	48.9	44.0	13.5	8.1	10.8	8.9	10.1	14.2	12.8
Pb	55.2	70.1	63.8	69.7	69.7	66.9	67.2	66.3	67.1	72.5	115.0	80.4	76.3	75.6	78.1	80.9
Rb	410	370	372	356	256	308	325	351	352	280	264	224	283	284	295	294
Sn	8.50	6.10	9.70	8.10	8.10	7.40	7.50	7.70	4.40	9.00	11.00	9.00	5.90	9.20	7.00	7.30
Sr	505	489	450	493	493	411	513	577	572	353	278	389	432	403	503	488
Th	47.2	53.8	49.3	49.6	49.6	54.7	52.1	59.3	48.6	49.7	59.3	53.2	49.2	48.2	49.2	49.3
U	-	-	-	-	-	-	-	-	-	-	-	-	-	-	-	-
V	118	95.5	91.3	91.4	91.4	96.9	90.4	89.5	88.0	66.1	61.8	71.9	72.3	74.2	79.0	74.5
Y	27.3	33.1	28.2	31.9	31.9	34.0	28.5	25.5	29.5	30.1	19.6	26.7	28.7	30.0	27.8	28.8
Zn	72.4	67.8	59.4	65.6	65.6	71.6	62.6	62.0	63.8	69.3	59.7	57.9	59.3	61.2	58.6	60.4
Zr	355	353	315	333	333	331	302	313	327	254	289	272	244	230	229	237
Hf	-	-	-	-	-	-	-	-	-	-	-	-	-	-	-	-
La	85.9	137	83.9	125	117	-	81.5	125	187	119	91.2	91.7	90.0	102	104	84.7
Ce	198	193	176	188	236	-	166	253	339	194	168	189	172	193	200	165
Pr	22.5	30.8	20.6	28.3	28.2	-	19.2	28.1	42.3	24.2	18.8	20.25	18.5	21.7	21.3	17.6
Nd	90.8	121	82.7	110	110	-	75.4	108	165	92.5	69.9	72.5	69.5	80.4	79.1	65.8
Sm	14.8	18.6	13.6	17.3	17.1	-	12.3	16	25.4	14.1	11.4	10.3	11.2	13.0	12.5	10.9
Eu	2.60	2.90	2.25	2.80	3.00	-	2.05	2.55	4.30	2.05	1.75	0.90	1.95	2.00	2.15	1.85
Gd	10.7	13.0	9.75	12.1	12.4	-	9.2	11.8	19.2	11.2	8.85	8.10	8.85	10.2	9.80	8.65
Tb	1.30	1.60	1.25	1.45	1.50	-	1.15	1.35	2.30	1.45	1.15	0.95	1.15	1.35	1.25	1.10
Dy	5.65	6.70	5.50	6.35	6.60	-	5.25	5.80	9.75	6.55	5.30	4.25	5.05	6.30	5.75	5.30
Ho	0.95	1.10	1.00	1.05	1.10	-	0.90	1.00	1.70	1.15	0.95	0.70	0.95	1.15	1.00	0.95
Er	2.70	3.05	2.70	2.90	3.05	-	2.60	2.70	4.65	3.25	2.60	1.90	2.60	3.20	2.85	2.65
Tm	0.35	0.40	0.35	0.35	0.40	-	0.35	0.35	0.60	0.40	0.35	0.25	0.35	0.40	0.40	0.35
Yb	2.35	2.45	2.40	2.30	2.60	-	2.80	2.30	3.85	2.75	2.20	1.50	2.30	2.80	2.45	2.15
Lu	0.35	0.30	0.20	0.35	0.40	-	0.35	0.30	0.35	0.12	0.12	0.35	0.35	0.40	0.13	0.12

All Fe as Fe_2O_3

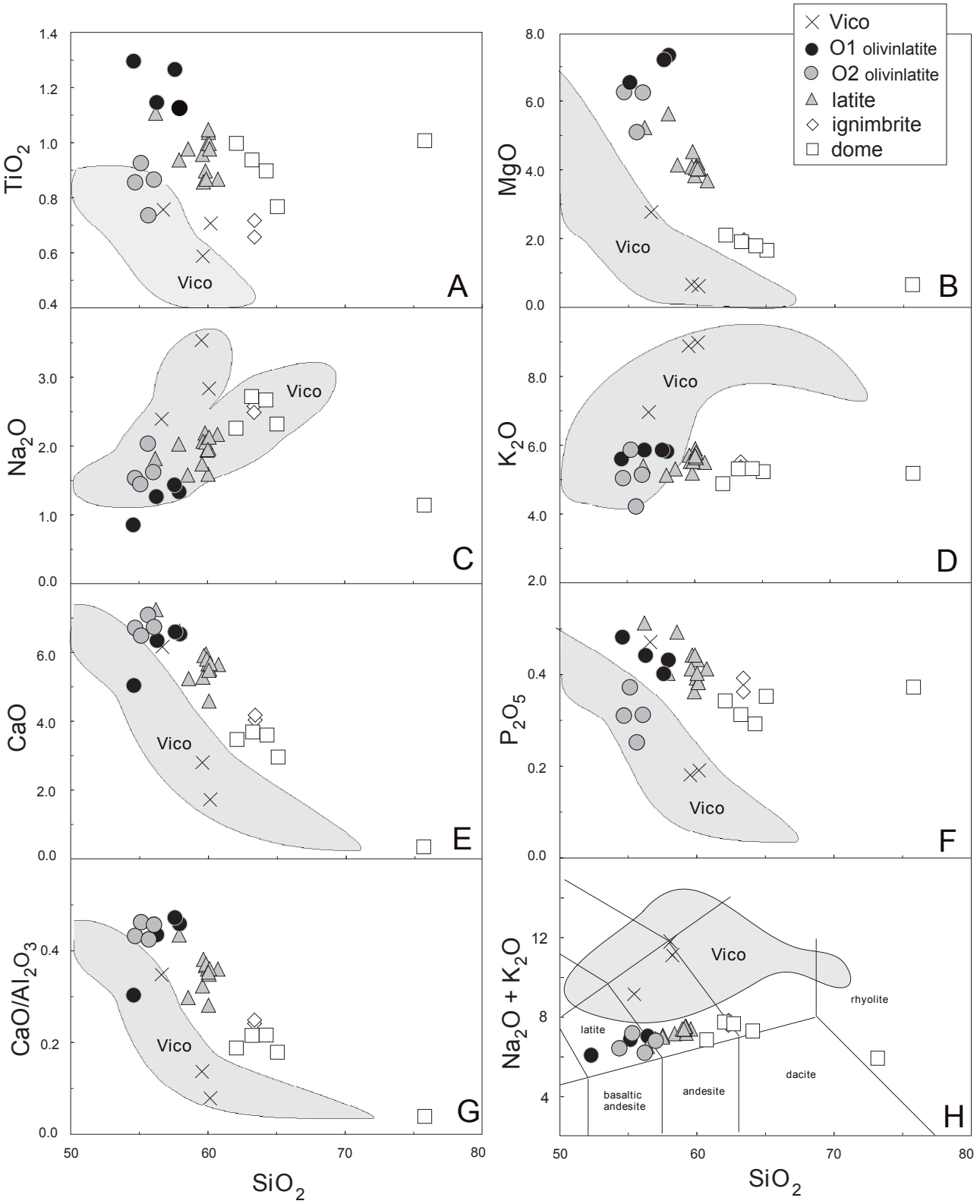

FIGURE 6 | **SiO_2 against major element (wt.%; A-F), CaO vs. Al_2O_3 (wt.%; G) variations and T.A.S. classification (H; Le Maitre et al., 2002) of Mts. Cimini volcanic rocks compared to Vico magmas (this work and D. Gasperini's unpublished data as grey fields).**

As recorded in several volcanic centers of the RMP, the most evolved samples are the oldest magmatic products, whereas most primitive magmas are erupted at the end of the volcanic history, usually after pyroclastic activity and caldera collapse (Conticelli et al., 2008). Several hypotheses can be put forward to explain such a typical eruptive sequence, such as stagnation of magma batches in shallow magmatic chambers and their consequent chemical and petrographic zoning (e.g., Blake 1981; Sparks et al. 1984; Perini et al. 2000; Kuritani 2001; Troll and Schmincke, 2002; Bryan, 2006). Upwelling of mafic magmas, decompression, and crustal faulting, may have followed reservoir emptying (due to ignimbrite phase) and collapse of the volcanic apparatus (e.g., Roche and Druitt, 2001; Gasperini, 2003; Holohan et al. 2005; Kennedy and Stix, 2007).

If early volcanic compositions at Mts. Cimini can be interpreted as the result of shallow magma differentiation, the origin of the heterogeneity of late olivinlatitic products is still a matter of debate. They show relatively

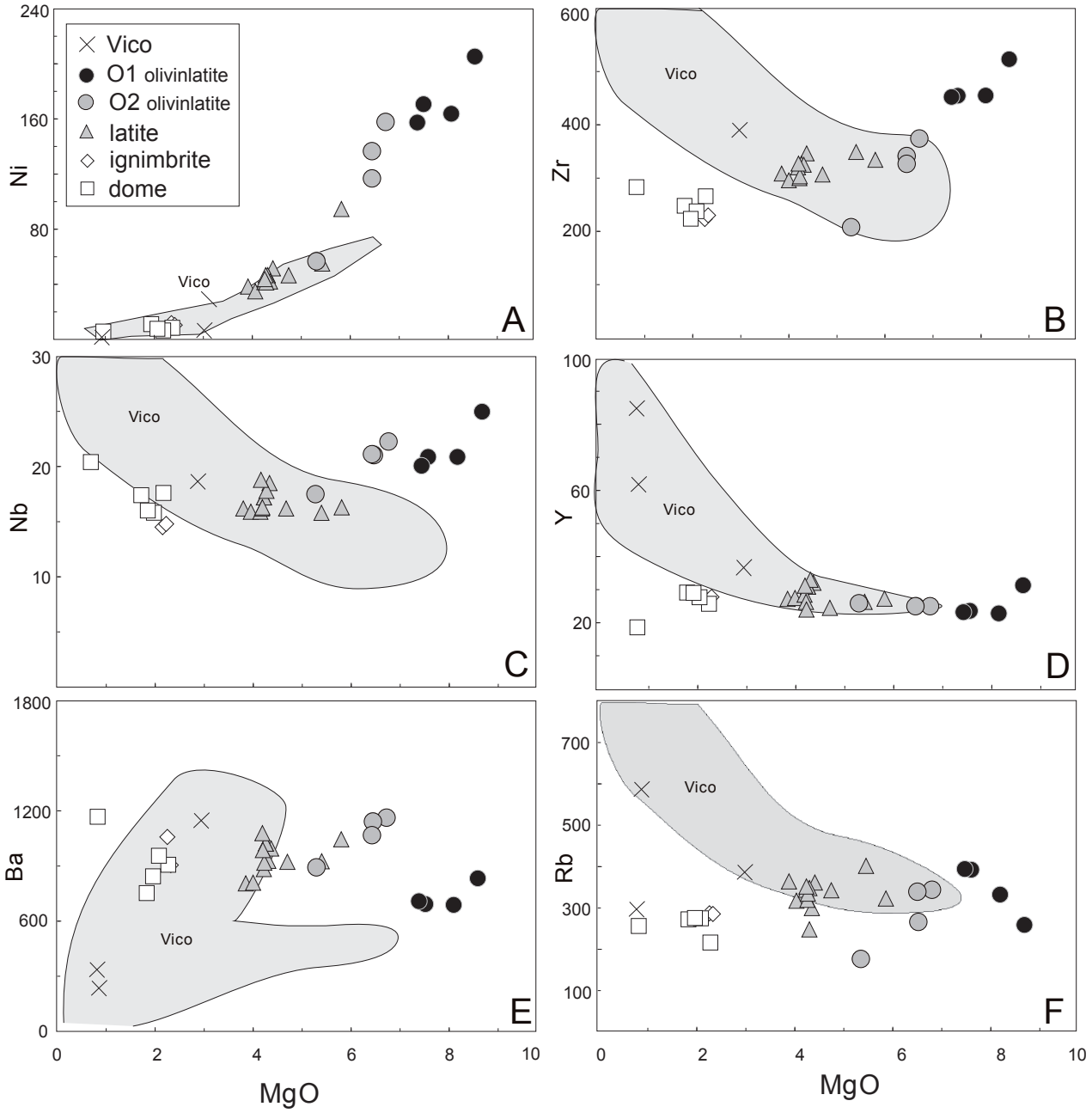

FIGURE 7 | **MgO content (wt.%) vs. trace element abundances (µg/g) for Mts. Cimini and Vico volcanic rocks (fields as in Fig. 6).**

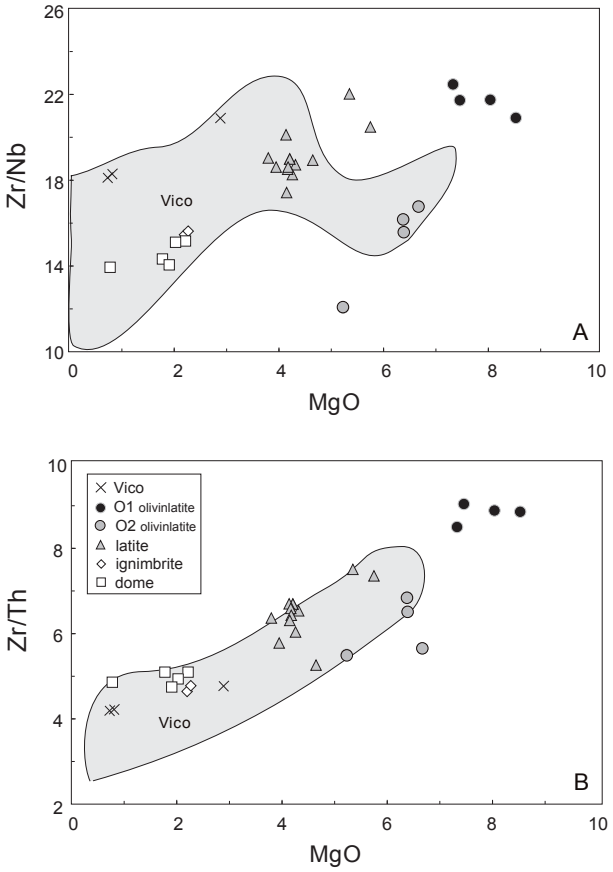

FIGURE 8 | **MgO content (wt.%) vs. A) Zr/Nb and (B) Zr/Th ratios of the analyzed rocks. Fields as in Fig. 6.**

homogeneous SiO_2, CaO and MgO (and Mg#) contents, but differ for incompatible element contents and Sr-isotope compositions. This geochemical signature in mafic magmas reflects a primary characteristic of their mantle source, and is probably related to heterogeneity and/or the effect of mixing/mingling events.

In summary, two groups of olivinlatites can be identified on the basis of their composition:

O1-type is characterized by high MgO, HFSE, HREE, Ti and P content, high incompatible element (Zr/Nb, Zr/Th, etc.) and $^{87}Sr/^{86}Sr$ values. These samples seem to represent the primitive magmas of most of Mts. Cimini products.

O2-type is characterized by lower MgO, HFSE, HREE, Ti and P content, and lower incompatible element (e.g., Zr/Nb, Zr/Th) and $^{87}Sr/^{86}Sr$ values. These samples are similar to those of the RMP (e.g., Vico and Vulsini; Gasperini et al., 2002; Gasperini, 2003).

O1 and O2 olivinlatites are also different in mineral chemistry and petrographic features. O2 is characterized by the presence of reversely zoned clinopyroxenes, with green cores showing compositional similarity to Vico and, more generally, to the Roman-type clinopyroxenes (Figs. 3-5). In contrast, clinopyroxenes of the O1 olivinlatites are similar to those occurring in Tuscan lamproites (Figs. 3-5).

Green clinopyroxene cores could be interpreted as cognate phases (e.g, Borley et al., 1971; Wilkinson, 1975) or cognate crystals (Brooks and Printzlau, 1978). Experimental studies have shown that a decrease in water pressure (P_{H2O}) affects clinopyroxene composition, thus resulting in a decrease of Fe^{3+} and Al in the tetrahedral site and a correspondent increase in Mg and Si content (Dolfi and Trigila, 1983, and references therein). Perini and Conticelli (2002) suggested that variations in P_{H2O} are related to a rapid degassing during magma eruption, and used this interpretation to explain the reversely zoned clinopyroxenes of the first period of the Vico volcanic activity. In the case of Mts. Cimini, the coexistence of homogeneous and reversely zoned clinopyroxenes,

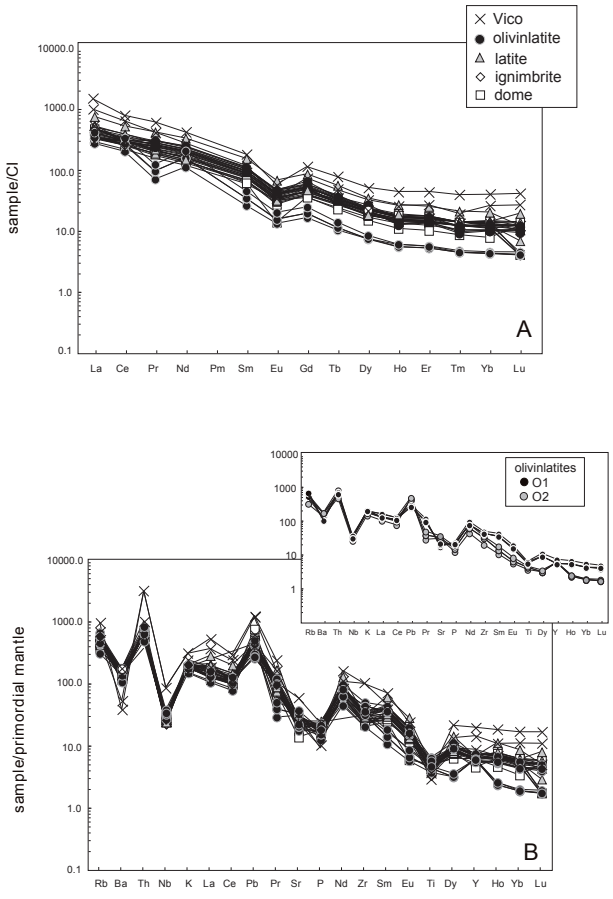

FIGURE 9 | **A) Cl-normalized (Sun and McDonough, 1989) REE patterns for Mts. Cimini volcanic rocks compared to the analyzed Vico samples; B) Primordial mantle-normalized (McDonough and Sun, 1995) trace element variation diagrams for the study bulk-rock samples. In the insert, the multielement-diagram of O1 and O2 is reported for comparison.**

TABLE 7 | **Sr, Nd and Pb isotope compositions for the volcanic rocks of Mts. Cimini and Vico**

Unit	Lava domes	2 σ	Lava domes	2 σ	ignimbrite	2 σ	Latitic lavas	2 σ	Latitic lavas	2 σ
Sample	MP10		MP6		CH5		MC6		MC7	
$^{87}Sr/^{86}Sr$	0.7139974*	0.000014	0.713944	0.000010	0.7136908*	0.000012	0.713507*	0.000018	0.713450	0.000010
$^{143}Nd/^{144}Nd$	0.5121216*	0.000010	0.512120	0.000006	0.5121339*	0.000014	n.d.	0.000008	0.512107	0.000006
$^{206}Pb/^{204}Pb$			18.705	0.001					18.726	0.001
$^{207}Pb/^{204}Pb$			15.665	0.001					15.687	0.001
$^{2083}Pb/^{204}Pb$			38.937	0.001					39.019	0.001

Unit	Olivinlatitic lavas	2 σ	Olivinlatitic lavas	2 σ	Olivinlatitic lavas	2 σ	Olivinlatitic lavas	2 σ	Vico lavas	2 σ	Vico lavas	2 σ
Sample	C6		C7		C8		C11		MP11		V1	
$^{87}Sr/^{86}Sr$	0.7156853*	0.000016	0.715228	0.000010	0.713480	0.000010	0.712180	0.000010	0.710778*	0.000012	0.711018	0.000012
$^{143}Nd/^{144}Nd$	0.512053*	0.000030	0.512054	0.000006	0.512098	0.000006	0.512142	0.000006	0.5121073*	0.000012	0.512109	0.000006
$^{206}Pb/^{204}Pb$			18.719	0.001	18.716	0.001	18.712	0.001			18.730	0.001
$^{207}Pb/^{204}Pb$			15.686	0.001	15.666	0.001	15.666	0.001			15.673	0.001
$^{2083}Pb/^{204}Pb$			39.018	0.001	38.938	0.001	38.948	0.001			38.979	0.001

Sr and Nd isotope ratios were analyzed at C.A.I. (Spain) with exception of those with * which were analyzed at SOCFAC-UK

together with the lack of correlation between Mg, Si and Fe^{3+} and ^{IV}Al in most of the analyzed samples, requires the occurrence of additional processes other than P_{H2O} variation during magma ascent. Changes in the oxidation state in the melt system can also be invoked to explain the Fe depletion in the rims of O2 clinopyroxenes. In fact, small changes in oxygen fugacity can bring about major changes in mineralogy (i.e., oxides crystallization), which in turn can change the path of magmatic fractionation. However, the similar composition between green clinopyroxene cores and clinopyroxenes from Vico (Roman-type) cannot exclude a xenocrystic origin for the O2 reverse zoned clinopyroxenes.

Melting of heterogeneous mantle sources (Conticelli et al., 1992, 2002, 2008) or simple mixing between mantle and crustal-derived magmas (Innocenti et al., 1992; Poli et al., 1984) were invoked to interpret geochemical variation in Mts. Cimini olivinlatites. An alternative hypothesis was proposed by Perini et al. (2003) who proposed that the geochemical variations within the olivinlatites cannot be generated by simple binary mixing between high Sr-radiogenic lamproite and trachyte end-members. The olivinlatites are K-rich and point to a high Sr-radiogenic lamproite-like magmas from the TMP, and their geochemical variability might have been induced by incorporation of K-feldspar megacrystals, previously crystallized in a Mts. Cimini trachytic magma. This mixing/mingling lowers the $^{87}Sr/^{86}Sr$ values and the incompatible trace element contents of the lamproitic ultrapotassic magma, which generated the isotopic and geochemical variations of the olivinlatites at Mts. Cimini. Perini et al. (2003) noted that among olivinlatites, modal content of K-feldspar megacrystals and Sr-isotope values are inversely correlated, and that all these xenocrysts are in isotopic disequilibrium with the bulk-rock composition. In addition, the Sr-Ba enrichment observed in olivinlatites (that is a tracer of the presence of K-feldspar in magmatic products) is negatively correlated with Sr-isotope ratios, thus supporting this hypothesis. In this case, the primitive magma of Mts. Cimini should correspond to the most Sr-radiogenic olivinlatites (here defined as O1-type group), not modified by mixing/mingling processes, as O2-type group instead were. By contrast, significant differences in ratios of highly incompatible trace elements which do not characterize K-feldspar composition, require an alternative or additional explanation to the hypothesis of K-feldspar incorporation.

Geochemical and isotopic variability have been found in most of the mafic rocks of volcanic centers of the RMP and interpreted as the result of mantle heterogeneity beneath Latium and Tuscany (Conticelli et al., 1992, 2002; Gasperini et al., 2002; Innocenti et al., 1992). Mts. Cimini are located in the proximity of Vico, which is believed to have reactivated the Mts. Cimini magmatic system (Perini et al., 2000). The occurrence of a common but heterogeneous mantle source for the two petrologically distinct volcanoes can not be ruled out. In accord with mass-balance calculations, we consider O1 olivinlatites as the most primitive magmas at Mts. Cimini, derived from a TMP-like mantle source, in which lamproitic geochemical features appear as predominant with respect to HKCA components (e.g., Conticelli et al., 2002; Perini et al., 2003). This is supported by the chemical composition of O1 clinopyroxenes, which are similar to lamproitic ones. In contrast, derivation of evolved Mts. Cimini products (lavas and ignimbrites) from O2 olivinlatites cannot be properly modeled. Fractional crystallization of O2 type

could generate geochemical compositions compatible to those of relatively evolved rocks from Vico volcano (trachyandesites).

The Mts. Cimini olivinlatites as a whole show a range of chemical variation that overlaps with that of the most mafic volcanics of the RMP (Fig. 11a), suggesting partial melting of similarly heterogeneous mantle sources for the two volcanic suites. O2 olivinlatites show Sr-isotope compositions which are intermediate between those of O1 (as TMP-like source) and the RMP primitive magmas (Fig. 11b). In the plot of K_2O content versus Zr/Nb, O2 type falls at the convergence

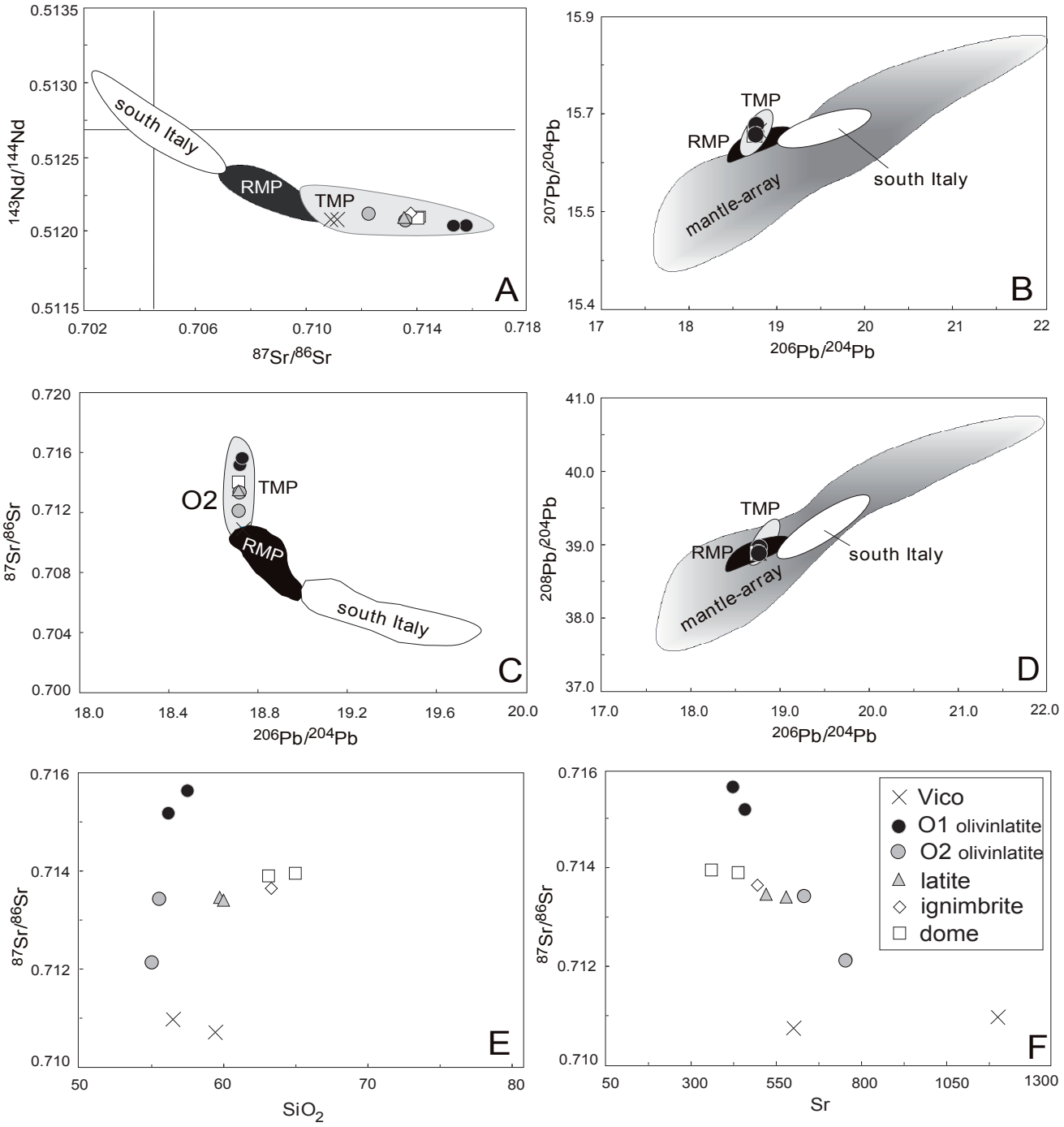

FIGURE 10 | **A-D) Sr, Nd and Pb isotope correlations for Mts. Cimini and Vico rocks, compared to the range of variations of the whole Italian magmatism (South Italy: Aeolian Islands, Etna, Iblean Basin; RMP: Roman Magmatic Province; TMP: Tuscan Magmatic Province; Gasperini et al. 2002). The mantle array is from literature data (Lehnert et al., 2000); C) SiO_2 content (wt.%) and d) Sr (µg/g) vs. Sr isotope ratios for the study volcanics. Fields as in Fig. 6.**

of both the field of variation of the RMP and Mts. Cimini (Fig. 11c).

When compared to the most primitive magmas of the RMP, the O2 olivinlatites show multi-element patterns and enrichment levels which are similar to the nearby volcanic centers from the RMP (namely Vulsini and Vico), although they are characterized by larger Pb-enrichment and HREE depletion. Finally, different fractionation of HREE in the two olivinlatitic suites suggest partial melting involving different mineral association and/or the occurrence of distinct or heterogeneous mantle sources.

We propose that both O1 and O2 olivinlatite magmas represent Mts. Cimini source compositions. The coexistence of these different magma types in the same volcanic center is ascribed to mantle heterogeneity which manifests itself in Tuscany and Latium, thus reflecting differently enriched portions of the same mantle region. Such geochemical heterogeneity could have been induced by deep mantle contribution, channeled into the Roman and Tuscan Provinces through a plate window in the subducted Adria plate, and interacting with the local mantle wedge since at least 8Ma (Lucente et al., 1999; Meletti et al., 2000; Gasperini et al., 2002; Bell et al., 2004). Deep mantle material and lithospheric components (metasomatized mantle wedge, recycled continental crust, etc.) may not have been homogenized in the source, so that individual basic magmas inherited a geochemical signature reflecting the original heterogeneity of the source mantle, following the model of a "veined mantle" (Beccaluva et al., 2004) or a "marble cake mantle" (Meibom and Anderson, 2003; Armienti and Gasperini, 2007).

The presence of material with geochemical features similar to OIB (Ocean Island Basalts) beneath central Italy and, more generally, Europe and central Mediterranean, has been recently related to a late Cretaceous contamination of

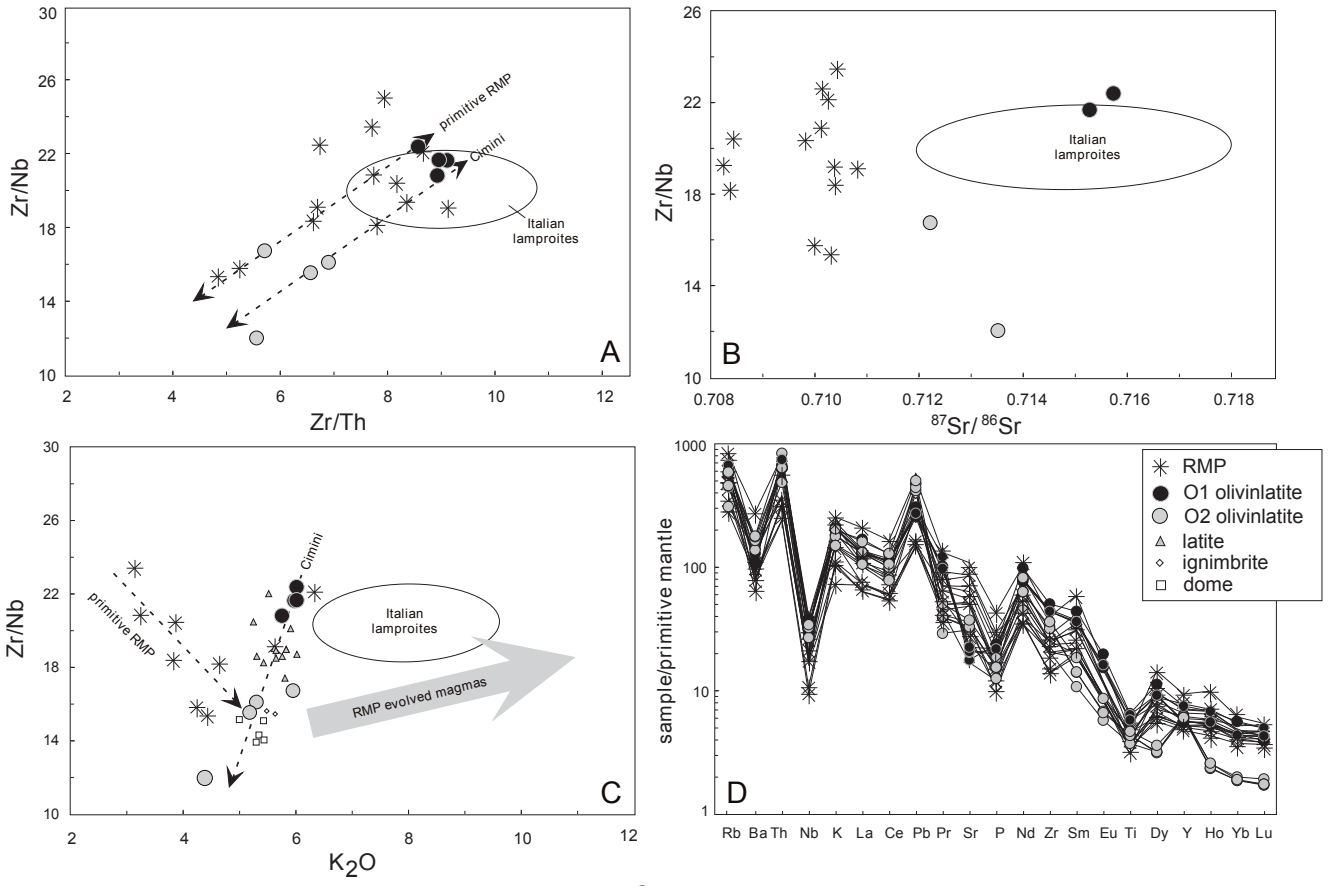

FIGURE 11 | **Comparison of A) Zr/Th ratios, B) Sr isotope, C) K_2O content vs. Zr/Nb ratios between Mts. Cimini olivinlatites and the most mafic volcanics of the RMP. The Mts. Cimini olivinlatites show a range of chemical variation which overlaps that of the RMP. O2 olivinlatites show Sr-isotope compositions and K_2O content which are intermediate between those of O1 and the RMP primitive magmas; D) Primordial Mantle-normalized (McDonough and Sun, 1995) trace element variation diagrams for the study olivinlatites compared to the most mafic magmas of the RMP (Gasperini et al., 2002). The patterns of the most mafic magmas of the TMP overlap with those of the O1 olivinlatites and were not reported for clarity. The field for the Italian lamproites is from Conticelli et al., 2009.**

the Euro-Mediterranean mantle. This was triggered by the rise of the Central Atlantic Plume head, at the time in which the Euro-Mediterranean region was located in proximity of such hot spot location (about 100Ma ago; Piromallo et al., 2008).

Geochemical and petrographic variation in the mantle source of Mts. Cimini olivinlatites could record a transition from a "typical" TMP- (O1) to a RMP-like (O2) mantle source. In this view, the last phase of activity of Mts. Cimini might mark a fundamental change of the heterogeneous mantle portion undergoing partial melting, thus shifting towards a mantle region with geochemical and petrographic features which are typical of the following magmatic activity in central Italy. The early Roman-type magma batches could have also mixed/mingled with the Tuscan-type primitive magmas, before becoming predominant. In this scenario, the TMP and RMP could keep their different identity, although fading to one another in terms of chemical and petrographic composition during the evolution of Mts. Cimini volcanism, and in its last phase of activity in particular. The transition from the TMP to the RMP magmatism likely started about 0.9Ma ago, during the emplacement of the olivinlatites (Nicoletti, 1969). The presence of leucite-free silicic rocks also in the first period of Vico activity (Perini et al., 2000) would suggest a transition for about 500ka, before the disappearance of the Tuscan-type magma contribution. Local scale compositional heterogeneity of the mantle source of both the TMP and RMP could imply that parental magmas are derived either from the same mantle depth or reflect the arrival of melts from further down.

CONCLUSIONS

Olivinlatites of Mts. Cimini erupted over the last phase of activity of this volcanic complex and show characteristic petrographic and geochemical features. In particular, two different main types of olivinlatites characterize the primitive magmas at Mts. Cimini. This heterogeneity may be related to a lithospheric mantle that was cross-cut by metasomatic veins or showed a "marble-cake" structure, located beneath Tuscany and Latium, and caused by the complex tectonic history of central Apennine since Oligocene (Meletti et al., 2000). In this scenario, partial melting took place in different places and times of the same heterogeneous mantle, i.e., the TMP and the RMP mantle sources. According to our data, the final activity at Mts. Cimini (about 900ka ago) records a transition from a TMP-like to an RMP-like mantle-derived magmas, allowing to recognize and explain the coexistence of both the geochemical signatures, e.g., calc-alkaline/lamproites and silica-undersaturated ultrapotassic affinities, in close spatial and temporal association.

ACKNOWLEDGMENTS

This work has been carried out in the framework of the Research Consolidated Group SGR-2009-972 PEGEFA (Applied and Basic Petrology and Geochemistry) recognized by AGAUR, Generalitat de Catalunya, and partially funded by the CGL2007-63727 project of the Spanish Government. Isotopic analyses benefited from analytical facility (2002) at Southampton Oceanographic Center (SOCFAC-UK) through an European Commision/ Research Infrastructure and additional funds from ACES00073 project, DURSI, Generalitat de Catalunya (2002). Preliminary field work was sustained by ACES98-57/6, DURSI, Generalitat de Catalunya (1999-2000) and institutional funds of University of Barcelona (1999). F. Costa is thanked for editorial handling and, together with G. Bianchini and an anonymous journal reviewer, for careful and insightful comments that significantly improved the manuscript. Donatella de Rita, Ciro Giampaolo, Sergio Lo Mastro and Guido Giordano of the University of Roma 3 (Italy) for introducing MA to the Mts. Cimini volcanic geology, as well as for their advice and help on sample collection; MA benefited of an ERASMUS grant in a very early phase of the work (1999); Rex Taylor and Andy Milton of SOCFAC-UK and the staff of the Serveis Científico-Tècnics of the Universitat de Barcelona for their support for sample analysis are acknowledged.

REFERENCES

Argnani, A., Savelli,. C., 1999. Cenozoic volcanism and tectonics in the southern Tyrrhenian sea: space–time distribution and geodynamic significance. Geodynamics, 27, 409-432.

Armienti, P., Gasperini, D., 2007. Do we really need mantle components to define mantle composition? Journal of Petrology, 48, 693-709.

Aulinas, M., Gimeno, D., Cimarelli, C., De Rita, D., Giampaolo, C., Giordano, G., Lo Mastro, S., 2004. Estudio petrológico del volcanismo cuaternário de los Monti Cimini y el volcán de Vico, Lazio, Italia. Geotemas, 6(1), 147-148.

Avanzinelli, R., Lustrino, M., Mattei, M., Melluso, L., Conticelli, S., 2009. Potassic and ultrapotassic magmatism in the circum-Tyrrhenian region: the role of carbonated pelitic vs. pelitic sediment recycling at destructive plate margin. Lithos, 113, 213-227.

Barberi, F., Buonasorte, G., Cioni, R., Fiordelisi, A., Foresi, L., Iaccarino, S., Laurenzi, M.A., Sbrana, A., Vernia, L., Villa, I.M., 1991. Evoluzione stratigrafico-strutturale e vulcanismo Plio-Quaternario dell'area tosco-laziale. In: Evoluzione dei bacini neogenici e loro rapporti con il magmatismo Plio-Quaternario dell'area tosco-laziale. Pisa (Italy), Atti del Workshop, 7-9.

Barberi, F., Gandino, A., Gioncada, A., La Torre, P., Sbrana, A., Zenucchini, C., 1994. The deep structure of the Eolian arc (Filicudi–Panarea–Vulcano sector) in light of gravity magnetic and Volcanology data. Journal of Volcanology and Geothermal Research, 61, 189-206.

Bartole, R., 1995. The North Tyrrhenian-Northern Apennines post collisional system: constraints for a geodynamical mode. Terra Nova, 7, 7-30.

Beccaluva, L., Di Girolamo, P., Serri, G., 1991. Petrogenesis and tectonic setting of the Roman Volcanic Province, Italy. Lithos, 26, 191-221.

Beccaluva, L., Coltorti, M., Galassi, R., Macciotta, G., Siena, F., 1994. The Cainozoic calc-alkaline magmatism of the western Mediterranean and its geodynamic significance. Bollettino di Geofisica Teorica Applicata, 141-144, 293-308.

Beccaluva, L., Bianchini, G., Bonadiman, C., Siena, F., Vaccaro C., 2004. Coexisting anorogenic and subduction-related metasomatism in mantle xenoliths from the Betic Cordillera (southern Spain). Lithos, 75, 67-87.

Beccaluva, L., Bianchini, G., Coltorti, M., Siena, F., Verde, M., 2005. Cenozoic tectono-magmatic evolution of the central-western mediterranean: migration of an arc-interarc basin system and variations in the mode of subduction. In: Finetti, I. (ed.). Crop Project – Deep Seismic exploration of the Central Mediterranean and Italy. Elsevier Special Volume, 623-640.

Bell, K., Castorina, F., Lavecchia, G., Rosatelli, G., Stoppa, F., 2004. Is there a mantle plume below Italy? Eos, 85, 541-547.

Bertagnini, A., Sbrana, A., 1986. Il vulcano di Vico: stratigrafia del complesso vulcanico e sequenze eruttive delle formazioni piroclastiche. Memorie della Società Geologica Italiana, 35, 699-713.

Bellon, H., 1981. Chronologie radiométric (K–Ar) des manifestations magmatique autour de la Mediterranée Occidentale entre 33 et 1 Ma. In: Wezel, F.C. (ed.). Sedimentary Basin of Mediterranean Margins. Tectonoprint Bologna, 341-368.

Ben Othman, D., White, W.M., Patchett, J., 1989. The geochemistry of marine sediments, island arc magma genesis, and crust –mantle recycling. Earth and Planetary Science Letters, 94, 1-21.

Bianchini, G., Beccaluva, L., Siena, F., 2004. A reappraisal of ultra-alkaline Intra-Apennine Volcanism in Central-Southern Italy: evidence for subduction-modified mantle sources. Periodico di Mineralogia, LXXIII, 177-185.

Bianchini, G., Beccaluva, L., Siena, F., 2008. Post-collisional and intraplate Cenozoic volcanism in the rifted Apennines/Adriatic domain. Lithos, 101, 125-140.

Blake, S., 1981. Eruptions from zoned magma chambers. Journal of the Geological Society, 138, 281-287.

Borley, G.D., Suddaby, P., Scott, P., 1971. Some xenoliths from alkali rock of Tenerife, Canary Islands. Contributions to Mineralogy and Petrology, 31(2), 102-118.

Bryan, S.E., 2006. Petrology and geochemistry of the Quaternary caldera-forming phonolitic Granadilla eruption, Tenerife (Canary Islands). Journal of Petrology, 47, 1557-1589.

Brooks, C.K., Printzlau, I., 1978. Magma mixing in mafic alkaline volcanic rocks: the evidence from relict phenocryst phases and other inclusions. Journal of Volcanology Geothermal Research, 4, 315-331.

Castorina, F., Stoppa, F., Cundari, A., Barbieri, M., 2000. An enriched mantle source for Italy's melilitite-carbonatite association as inferred by its Nd-Sr isotope signature. Mineral Magmatology, 64(4), 625-639.

Cellai, D., Conticelli, S., Menchetti, S., 1994. Crystal-chemistry of clinopyroxenes from potassic and ultrapotassic rocks in central Italy: implications on their genesis. Contributions to Mineralogy and Petrology, 116, 301-315.

Cimarelli, C., De Rita, D., 2006. Structural evolution of the Pleistocene Cimini trachytic volcanic complex (Central Italy). Bulletin of Volcanology, 68, 538-548.

Cioni, R., Laurenzi, M.A., Sbrana, A., Villa, I., 1993. $^{40}Ar/^{39}Ar$ chronostratigraphy of the initial activity in the Sabatini volcanic complex (Italy). Bollettino della Società Geologica Italiana, 112, 251-263.

Civetta, L., Orsi, G., Scandone, P., Pece, R., 1978. Eastward migration of the Tuscan anatectic magmatism due to anticlockwise rotation of the Apennines. Nature, 276, 604-606.

Conticelli, S., 1998. The effect of crustal contamination on ultrapotassic magmas with lamproitic affinity: Mineralogical geochemical and isotope data from Torre Alfina and xenoliths central Italy. Chemical Geology, 149, 51-81.

Conticelli, S., Peccerillo, A., 1992. Petrology and geochemistry of potassic and ultrapotassic volcanism in central Italy: petrogenesis and inferences on the evolution of the mantle sources. Lithos, 28, 221-240.

Conticelli, S., Manetti, P., Menichetti, S., 1992. Petrology chemistry mineralogy and Sr-isotopic features of Pliocenic Orendites from south Tuscany: implications in their genesis and evolutions. European Journal of Mineralogy, 4, 1359-1375.

Conticelli, S., D'Antonio, M., Pinarelli, L., Civetta, L., 2002. Source contamination and mantle heterogeneity in the genesis of Italian potassic and ultrapotassic volcanic rocks: Sr-Nd-Pb isotope data from Roman Province and Southern Tuscany. Mineralogy and Petrology, 74, 189-222.

Conticelli, S., Guarnieri, L., Farinelli, A., Mattei, M., Avanzinelli, R., Bianchini, G., Boari, E., Tommasini, S., Tiepolo, M., Prelević, D., Venturelli, G., 2009. Trace elements and Sr–Nd–Pb isotopes of K-rich, shoshonitic, and calc-alkaline magmatism of the Western Mediterranean Region: genesis of ultrapotassic to calc-alkaline magmatic associations in a post-collisional geodynamic setting. Lithos, 107, 68-92.

Conticelli, S., Marchionni, S., Rosa, D., Giordano, G., Boari, E., Avanzinelli, R., 2008. Shoshonite and sub-alkaline magmas from an ultrapotassic volcano: Sr-Nd-Pb isotope data on the Roccamonfina volcanic rocks, Roman Magmatic Province, Southern Italy. Contributions to Mineralogy and Petrology, 157, 41-63.

Deer, W.A., Howie, R.A., Zussman, J., 1963. Rock-forming minerals. Chain silicates. London, Longmans London, 379pp.

Deer, W.A., Howie, R.A., Zussman, J., 1992. An introduction to the rock forming minerals. Essex, Longman, Harlow, 692pp.

Dolfi, D., Trigila, R., 1983. Clinopyroxene solid solutions and water in magmas: results in the system phonolitic tephrite-H_2O. Mineralogical Magazine, 47, 347-351.

Droop, G.T.R., 1987. A general equation for estimating Fe^{3+} concentrations in ferromagnesian silicates and oxides from microprobe analyses, using stoichiometric criteria. Mineralogical Magazine, 51, 431-435.

Ellam, R.M., Hawkesworth, C.J., Menzies, M.A., Rogers, N.V., 1989. The volcanism of Southern Italy: role of subduction and the relationship between potassic and sodic alkaline magmatism. Journal of Geophysical Research, 9, 4589-4601.

Ferrara, G., Giuliani, O., Tonarini, S., Villa, I.M., 1988. Datability and isotopic disequilibrium in anatectic volcanites from S. Vincenzo and Tolfa (Tuscany-Latium). Rendiconti della Società Italiana di Mineralogia e Petrografia, 7, 72.

Ferrara, G., Petrini, R., Serri, G., Tonarini, S., 1989. Petrology and isotope geochemistry of San Vincenzo rhyolites (Tuscany Italy). Bulletin of Volcanology, 51, 379-388.

Foley, S.F., Venturelli, G., Green, D.H., Toscani, L., 1987. The ultrapotassic rocks; characteristics classification and constraints for petrogenetic models. Earth Science Review, 24, 81-134.

Fornaseri, M., 1985. Geochronology of volcanic rocks from Latium and from Umbria. Rendiconti della Società Italiana di Mineralogia e Petrologia, 40, 73-106.

Frezzotti, M.L., De Astis, G., Dallai, L., Ghezzo, C., 2007. Coexisting calc-alkaline and ultrapotassic magmatism at Monti Ernici, Mid Latina Valley (Latium, central Italy). European Journal of Mineralogy, 19, 479-497.

Gasparon, M., Rosembaum, G., Wijbrans, J., Manetti, P., 2009. The transition from subduction arc to slab tearing: evidence from Capraia Island, northern Tyrrenian Sea. Journal of Geodynamics, 47, 30-38.

Gasperini, D., 2003. Il ruolo dei processi a bassa pressione nella petrogenesi del magmatismo pleistocenico della Provincia Magmatica Romana: dati isotopici preliminari sul vulcano di Vico. Rendiconti Lincei, Scienze Fisiche e Matematiche, 14, 161-177.

Gasperini, D., Blichert-Toft, J., Bosch, D., Del Moro, A., Macera, P., Albarède, F., 2002. Upwelling of deep mantle material through a plate window: evidence from the geochemistry of Italian basaltic volcanics. Journal of Geophysical Research, 107, B12, 2367-2385.

Giunchi, C., Sabadini, R., Boschi, E., Gasperini, P., 1996. Dynamic models of subduction: geophysical and geological evidence in the Tyrrhenian Sea. Geophysical Journal International, 126, 555-578.

Hickey, R.L., Frey, F.A., Gerlach, D.C., 1986. Multiple sources for basaltic arc rocks from the southern volcanic zone of the Andes (34–41°S): trace element and isotopic evidence for contribution from subducted oceanic crust, mantle and continental crust. Journal of Geophysical Research, 91, 5963-5983.

Hofmann, A.W., 1997. Mantle geochemistry: the message from oceanic volcanism. Nature, 385, 219-229.

Holohan, E.P., Troll, V.R., Walter, T.R., Münn, S., McDonnell, S., Shipton, Z.K., 2005. Elliptical calderas in active tectonic settings: an experimental approach. Journal of Volcanology and Geothermal Research, 144, 119-136.

Imai, N., Terashima, S., Itoh, S., Ando, A., 1995. 1994 compilation values for GSJ reference samples, Igneous Rock Series. Geochemical Journal, 29, 91-95.

Innocenti, F., Serri, G., Ferrara, G., Manetti, P., Tonarini, S., 1992. Genesis and classifications of the rocks of the Tuscan Magmatic Province: thirty years after Marinelli's model. Acta Vulcanologica, 2, 247-265.

Juteau, M., Michard, A., Albarède, F., 1986. The Pb–Sr–Nd isotope geochemistry of some recent circum-Mediterranean granites. Contributions to Mineralogy and Petrology, 92, 331-340.

Keller, J., 1983. Potassic lavas in the orogenic volcanism of the Mediterranean area. Journal of Volcanology and Geothermal Research, 18, 321-335.

Kennedy, B., Stix, J., 2007. Magmatic processes associated with caldera collapse at Ossipee ring dyke, New Hampshire. Geological Society of America Bulletin, 119, 3-17.

Kuritani, T., 2001. Replenishment of a mafic magma in a zoned felsic magma chamber beneath Rishiri Volcano, Japan. Bulletin of Volcanology, 62, 533-548.

La Berge, R., Cas, R.A.F., Giordano, G., Cimarelli, C., Phillips, D., 2004. Explosive emergence of a rhyodacite lava dome and the complex facies architecture of the resultant dense-clast and pumiceous pyroclastic flow deposits: the Pleistocene Cimino ignimbrite in northern Lazio, Italia. International Association of Volcanology and Chemistry of the Earth's Interior (IAVCEI), November 14-19, General Assembly Abstracts, Pucon-Chile, Geophysical Institute Library, University of Alaska, Fairbanks.

Lardini, D., Nappi, G., 1987. I cicli eruttivi del complesso vulcanico Cimino. Rendiconti della Società Geolgica Italiana di Mineralogia e Petrografia, 42, 141-153.

Laurenzi, M.A., Villa, I.M., 1985. KrAr chronology of the Vico volcanoLatium, Italy. International Association of Volcanology and Chemistry of the Earth's Interior (IAVCEI) September 16-21, General Assembly Abstracts, Giardini Naxos-Italy, Geophysical Institute Library, University of Alaska, Fairbanks.

Laurenzi, M.A., Villa, I.M., 1987. $^{40}Ar/^{39}Ar$ chronostratigraphy of Vico ignimbrites. Periodico di Mineralogia, 56, 285-293.

Le Maitre, R.W., Streckeisen, A., Zanettin, B., Le Bas, M.J., Bonin, B., Bateman, P., Bellieni, G., Dudek, A., Efremova, S., Keller, J., Lamere, J., Sabine, P.A., Schmid, R., Sorensen, H., Woolley, A.R., 2002. Le Maitre, R.W. (ed.). Igneous Rocks: A Classification and Glossary of Terms, Recommendations of the International Union of Geological Sciences, Subcommission of the Systematics of Igneous Rocks. Cambridge, Cambridge University Press, 236pp.

Lehnert, K., Su, Y., Langmuir, C., Sarbas, B., Nohl, U., 2000. A global geochemical database structure for rocks. Geochemistry Geophysics Geosystem 1, doi:10.1029/1999GC000026.

Lombardi, G., Nicoletti, M., Petrucciani, C., 1974. Età delle vulcaniti acide del complesso Tolfetano Cerite e Manziate (Lazio nord-occidentale). Periodico di Mineralogia, 43, 351-376.

Lucente, P.F., Chiarabb, C., Cimini, G.B., Giardini, D., 1999. Tomographic constraints on the geodynamic evolution of the

Italian region. Journal of Geophysical Research, 104, 20307-20327.

Marinelli, G., 1975. Magma evolution in Italy. In: Geology of Italy. Squyres, C.H. (ed). Earth Science Society of the Libian Arabian Republic. Tripoli, Libyan Arabian Republic (LAR), 165-219.

McDonough, W.F., Sun, F.F., 1995. The composition of the Earth. Chemical Geology, 120, 223-253.

Mattias, P.P., Ventriglia, V., 1970. La regione vulcanica dei Monti Sabatini e Cimini. Memorie della Società Geologica Italiana, 9, 381-384.

Meibom, A., Anderson, D.L, 2003. The statistical upper mantle assemblage. Earth and Planetary Science Letters, 217, 123-139.

Meletti, C., Patacca, E., Scandone, P., 2000. Construction of a seismotectonic model: the case of Italy. Pure Applied Geophysics, 157, 11-35.

Mittempergher, M., Tedesco, C., 1963. Some observations on the ignimbrites lava domes and lava flows of M. Cimino (Central Italy). Bulletin of Volcanology, 25, 343-358.

Morimoto, N., 1989. Nomenclature of pyroxenes. Canadian Mineralogy, 27, 143-156.

Nicoletti, M., 1969. Datazioni argon-potassio di alcune vulcanite delle regioni vulcaniche Cimina e Vicana. Periodico di Mineralogia, 38, 1-20.

Peccerillo, A., 1998. Relationships between ultrapotassic and carbonate-rich volcanic rocks in central Italy: Petrogenetic and geodynamic implications. Lithos, 43, 267-279.

Peccerillo, A., 1999. Multiple mantle metasomatism in central-southern Italy: geochemical effects, timing and geodynamic implications. Geology, 27, 315-317.

Peccerillo, A., 2002. Plio-Quaternary magmatism in central-southern Italy: a new classification scheme for volcanic provinces and its geodynamics implications. Bollettino della Società Geologica Italiana, 1(Special Volume), 113-127.

Peccerillo, A., 2005. Plio-Quaternary volcanism in Italy. Episodes, 26, 222-226.

Peccerillo, A., Manetti, P., 1985. The potassium alkaline volcanism of central Southern Italy: a review of the data relevant to petrogenesis and geodynamics significance. Transection of the Geological Society of South Africa, 88, 379-394.

Peccerillo, A., Conticelli, S., Manetti, P., 1987. Petrological characteristics and the genesis of the recent magmatismo of southern Tuscany and northern Latium. Periodico di Mineralogia, 56, 157-172.

Perini, G., Conticelli, S., 2002. Crystallization conditions of leucite-bearing magmas and their implications on the magmatological evolution of ultrapotassic magmas: the Vico volcano, central Italy. Mineralogy and Petrology, 74, 253-276.

Perini, G., Conticelli, S., Francalanci, L., 1997. Inferences on the volcanic history of the Vico volcano, Roman Magmatic Province, Central Italy: stratigraphic, petrographic and geochemical data. Mineralogica Petrografica Acta, 40, 67-93.

Perini, G., Conticelli, S., Francalanci, L., Davidson, J.P., 2000. The relationship between potassic and cac-alkaline post-orogenic magmatism at Vico volcano, central Italy. Journal of Volcanology and Geothermal Research, 95, 247-272.

Perini, G., Tepley III, F.J.T., Davidson, J.P., Conticelli, S., 2003. The origin of K-feldspar megacrystals hosted in alkaline potassic rocks from central Italy: a track for low-pressure processes in mafic magmas. Lithos, 66, 223-240.

Piromallo, C., Gasperini, D., Macera, P., Faccenna, C., 2008. A late Cretaceous contamination episode of the European–Mediterranean mantle. Earth and Planetary Science Letters, 268, 15-27.

Poli, G., Frey, F., Ferrara, G., 1984. Geochemical characteristics of the south Tuscany, Italy, volcanic province: constraints on lava petrogenesis. Chemical Geology, 43, 203-221.

Puxeddu, M., 1971. Studio chimico-petrografico delle vulcaniti del M Cimino (Viterbo). Atti della Società Toscana di Scienze Naturali, Serie A, 78, 329-394.

Roche, O., Druitt, T.H., 2001. Onset of caldera collapse during ignimbrite eruptions. Earth Planetary Science Letters, 191, 191-202.

Rogers, N.W., Hawkesworth, C.J., Parker, R.J., Marsh, J.S., 1985. The geochemistry of potassic lavas from Vulsini, central Italy, and implications for mantle enrichment processes beneath the Roman Region. Contributions to Mineralogy and Petrology, 90, 244-257.

Sabatini, V., 1912. I vulcani dell'Italia centrale e i loro prodotti. Parte seconda: Vulcani Cimini. Memorie Descrittive della Carta Geolica Italiana, 15, 617pp.

Scrocca, D., Doglioni, C., Innocenti, F., 2003. Constraints for an interpretation of the Italian geodynamics: a review. Memorie Descrittive della Carta Geologica d'Italia, LXII, 15-46.

Serri, G., 1997. Neogene-Quaternary magmatic activity and its geodynamic implications in the Central Mediterranean region. Annals of Geophysics, 40(3), 681-703.

Serri, G., Innocenti, F., Manetti, P., 1993. Geochemical and petrological evidence of the subduction of delaminated Adriatic continental lithosphere in the genesis of the Neogene–Quaternary magmatism of central Italy. Tectonophysics, 223, 117-147.

Sollevanti, F., 1983. Geologic volcanologic and tectonic setting of the Vico-Cimini area, Italy. Journal of Volcanology and Geothermal Research, 17, 203-217.

Sparks, R.S.J., Huppert, H.E., Turner, J.S., Sakuyama, M., O'Hara, M.J., 1984. The fluid dynamics of evolving magma chambers. Journal of Philosophical Transactions of the Royal Society, London, Series A, Mathematical and Physical Sciences (1934-1990), 310, 511-534.

Stormer, J.C., Nicholls, J., 1978. XLFRAC: a program for the interactive testing of magmatic differentiation models. Computer and Geoscience, 4, 143-159.

Sun, S.S., Mc Donough, W.F., 1989. Chemical and isotopic systematics of oceanic basalts: implications for mantle composition and processes. In: Saunders, A.D., Norris, M.J. (eds.). Magmatism in the ocean basins. London, Geological Society, Special Pubblications, 313-345.

Tamburelli, C., Babbucci, D., Mantovani, E., 2000. Geodynamic implications of ''subduction-related'' magmatism: Insights

from the Tyrrhenian-Apennines region. Journal of Volcanology and Geothermal Research, 104, 33-43.

Thorpe, R.S., Francis, P.W., O'Callaghan, L., 1984. Relative roles of source composition fractional crystallization and crustal contamination in the petrogenesis of Andean volcanic rocks. London, Philosophical Transactions of the Royal Society, Series A, 310, 675-692.

Todt, M., Cliff, R.A., Hauser, A., Hofmann, A.W., 1984. ^{202}Pb-^{205}Pb spike for Pb isotopic analysis. Terra Cognita, 4, 209.

Troll, V.R., Schmincke, H.-U., 2002. Magma mixing and crustal recycling recorded in ternary feldspar from compositionally zoned peralkaline ignimbrite A', Gran Canaria, Canary Islands. Journal of Petrology, 43, 243-270.

Wilkinson, J.F.G., 1975. Ultramafic inclusions and high pressure megacrystals from a nepehlinite sill, Nandewar Mountains, Northerneastern New South Wales, and their bearing on the origin of certain ultramafic inclusions in alkaline volcanic rocks. Contributions to Mineralogy and Petrology, 51, 235-262.

Wilson, M., 1989. Igneous Petrogenesis. New York, Chapman and Hall, 466pp.

Wortel, M.J.R., Spakman, W., 2000. Subduction and slab detachment in the Mediterranean–Carpatian region. Science, 290, 1910-1917.

Manuscript received November 2009;
revision accepted May 2010;
published Online October 2010.

Appendix: Analytical techniques

Major and trace elements, and Sr, Nd and Pb isotopes of whole-rock, as well as mineral chemistry analyses were carried out on samples representative of the different petrographic and chronological units of Mts. Cimini. The location of the selected samples is indicated in Table 1. Three samples from Vico were also analyzed for comparison.

Major element compositions of the phenocrysts were determined by Electron MicroProbe Analysis (EPMA) at the SCT-UB, using a Cameca SX 50 instrument. An acceleration voltage of 20kV and a current beam of 15 – 20nA were used in all the analyses with the exception of sodium. This element was analysed first in the sequence using a current of 6nA and an incident electron beam of 5 – 10μm diameter. The analysed elements were Si, Al, Ti, Mg, Ca, Na, K, P, Mn, Cr, Ni, Sr and Ba. Calibration of the instrument was done with reference materials consisting of natural and synthetic silicates and oxides with certified composition.

Prior to their elemental and isotopic analysis, samples were pulverized in an agate mills. Analysis of ignimbrite samples only include pumice clasts, which were separated from the rest of pyroclastic material previous to their processing.

Whole-rock XRF (X-ray fluorescence) major and trace elements analyses (except for REE, Hf and U) were performed using a sequential X-ray spectrometer Philips PW2400 at Serveis Cientificotècnics of the University of Barcelona (SCT-UB). Sample preparation for major elements consisted on producing duplicated pearls (with lithium borate 1:20) and pressed powder pellets, respectively. REE, Hf and U were analyzed by ICP-MS (inductively coupled plasma-mass spectrometry) at the SCT-UB. In this case, samples were attacked with an acid mixture of HNO_3-HF-$HClO_4$ (2.5:5:2.5ml). The precision and accuracy of XRF and ICP-MS measurements were monitored using reference materials of the Geological Survey of Japan (JA-3 for major elements and JB-3 for REE, Hf and U; Imai et al., 1995) and by an XRF internal reference material (GSS-8) for XRF trace elements. For major elements, the precision (2σ RSD, n=4) is better than 3.0% with exception of SiO_2 (6.5%) and MnO and P_2O_5 (up to 10%), whereas accuracy is better than 2% for all major elements with exception of P_2O_5 (up to 5%). XRF trace element precision (2σ RSD, n=10) is better than 8% for all elements. ICP-MS trace elements (REE, Hf and U) precision (2σ RSD, n=4) is better than 9%, and accuracy is better than 5% for all elements. Loss on ignition (LOI) was determined by heating samples at 95ºC during four hours. Several LOI values are negative because of Fe oxidation and low H_2O content.

Sr and Nd isotope ratios were measured on eleven samples using a Micromass VG-Sector 54 TIMS in two different institutions, the Centro de Geocronología y Geoquímica Isotópica, Universidad Complutense de Madrid, Spain (CAI) and the SOCFAC, Southampton University, UK. Lead isotope ratios were determined using a Triton Thermal Ion Mass Spectrometer (TIMS) at the Carleton University, Canada. The whole-rock samples were analysed in two sessions at CAI, during which NBS 987 was 0.710237 ± 0.00004 and 0.710248 ± 0.00002 (2σ; n=15 and 10, respectively). In the case of SOCFAC analyses, samples were analysed in one session during which the average $^{87}Sr/^{86}Sr$ value for NBS 987 was 0.710250 ± 0.00001 (2σ; n=4). For each session, the average $^{143}Nd/^{144}Nd$ value for La Jolla standard was 0.511824 ± 0.00003 (2σ; n=8) and 0.511862 ± 0.00003 (2σ; n=10) at the CAI. $^{143}Nd/^{144}Nd$ value for JindM standard was 0.512099 ± 0.00001 (2σ; n=4) at SOCFAC. Lead isotope ratios were measured in one session on six whole-rock samples. All mass spectrometer runs were corrected for mass fractionation using reference material. Reproducibility for $^{206}Pb/^{204}Pb$, $^{207}Pb/^{204}Pb$, and $^{208}Pb/^{204}Pb$ for standard NBS 981 was 16.892 ± 0.010, 15.431 ± 0.013, and 36.512 ± 0.010 (2σ; n=20), respectively. The fractionation correction, based on the values of Todt et al. (1984), was +0.13% / amu. The Sr, Nd and Pb blank values were negligible for the analyzed samples during the period of measurements.